Synthesis and Characterization of Enantiomerically Pure *cis*- and *trans*-3-Fluoro-2,4-dioxa-9-aza-3-phosphadecalin 3-Oxides as Acetylcholine Mimetics and Inhibitors of Acetylcholinesterase

by **Piergiorgio Lorenzetto**, **Michael Wächter**, and **Peter Rüedi***

Organisch-chemisches Institut der Universität Zürich, Winterthurerstrasse 190, CH-8057 Zürich (phone: +41-44-8215579; e-mail: peru@oci.uzh.ch)

Dedicated to Professor *Heinz Heimgartner* on the occasion of his 70th birthday

The title compounds, the *P(3)*-axially and *P(3)*-equatorially substituted *cis*- and *trans*-configured 9-benzyl-3-fluoro-2,4-dioxa-9-aza-3-phosphadecalin 3-oxides (= 9-benzyl-3-fluoro-2,4-dioxa-9-aza-3-phosphabicyclo[4.4.0]decane 3-oxides = 7-benzyl-2-fluorohexahydro-4*H*-1,3,2-dioxaphosphorino[4,5-*c*]pyridine 2-oxides) were prepared (ee >99%) and fully characterized (*Schemes 2* and *4*). The absolute configurations were deduced from that of their precursors, the enantiomerically pure ethyl 1-benzyl-3-hydroxypiperidine-4-carboxylates and 1-benzyl-3-hydroxypiperidine-4-methanols which were unambiguously assigned. Being configuratively fixed and conformationally constrained phosphorus analogues of acetylcholine, the title compounds represent acetylcholine mimetics and are suitable probes for the investigation of molecular interactions with acetylcholinesterase. As determined by kinetic methods, all of the compounds are moderate irreversible inhibitors of the enzyme.

1. Introduction. – In the course of our research project concerning the synthesis of configuratively fixed and conformationally constrained organophosphates as inhibitors of acetylcholinesterase (AChE) and related serine hydrolases (*e.g.*, chymotrypsin), we have reported on the preparation and characterization of the racemic *P(3)*-axially and *P(3)*-equatorially substituted *cis*- and *trans*-2,4-dioxa-9-aza- (**I**), *cis*- and *trans*-2,4-dioxa-8-aza- (**II**), and *cis*- and *trans*-2,4-dioxa-7-aza-3-phosphadecalin 3-oxides (**III**) [1]. The first enantiomerically pure 2,4-dioxa-3-phosphadecalin 3-oxides (**IV**, L = F [2], L = 2,4-dinitrophenoxy [3] and the corresponding (1,5,5-$^2H_3$)-isomers [4]) have been presented, too (*Scheme 1*). Being P-analogues of acetylcholine (7-aza- and 9-aza isomers) or γ-homoacetylcholine mimetics (8-aza isomers), the compounds are considered to be suitable probes for the investigation of molecular interactions with the enzyme, such as the recognition conformation of acetylcholine (=2-(acetyloxy)-*N*,*N*,*N*-trimethylethanaminium; ACh) [5] and the stereochemical course of the inhibition reaction [3][4]. In this report, we discuss the synthesis and full characterization of the first enantiomerically pure 9-benzyl-3-fluoro-2,4-dioxa-9-aza-3-phosphadecalin 3-oxides (= 9-benzyl-3-fluoro-2,4-dioxa-9-aza-3-phosphabicyclo[4.4.0]decane 3-oxides = 7-benzyl-2-fluorohexahydro-4*H*-1,3,2-dioxaphosphorino[4,5-*c*]pyridine 2-oxides) **14** and **15** representing type-**I** inhibitors. In this context, we also give a full account on the absolute configurations and the chiroptical data of their presursors, ethyl *trans*- and *cis*-1-benzyl-3-hydroxypiperidine-4-carboxylates ((+)- and (−)-**2** and (+)- and (−)-**3**, resp.) and *trans*- and *cis*-1-benzyl-3-hydroxypiperidine-4-methanols

((+)- and (−)-**8** and (+)- and (−)-**9**, resp.) as partly presented in a previous report to clear fundamental structural inconsistencies in the current literature [6][1]).

Scheme 1[a])

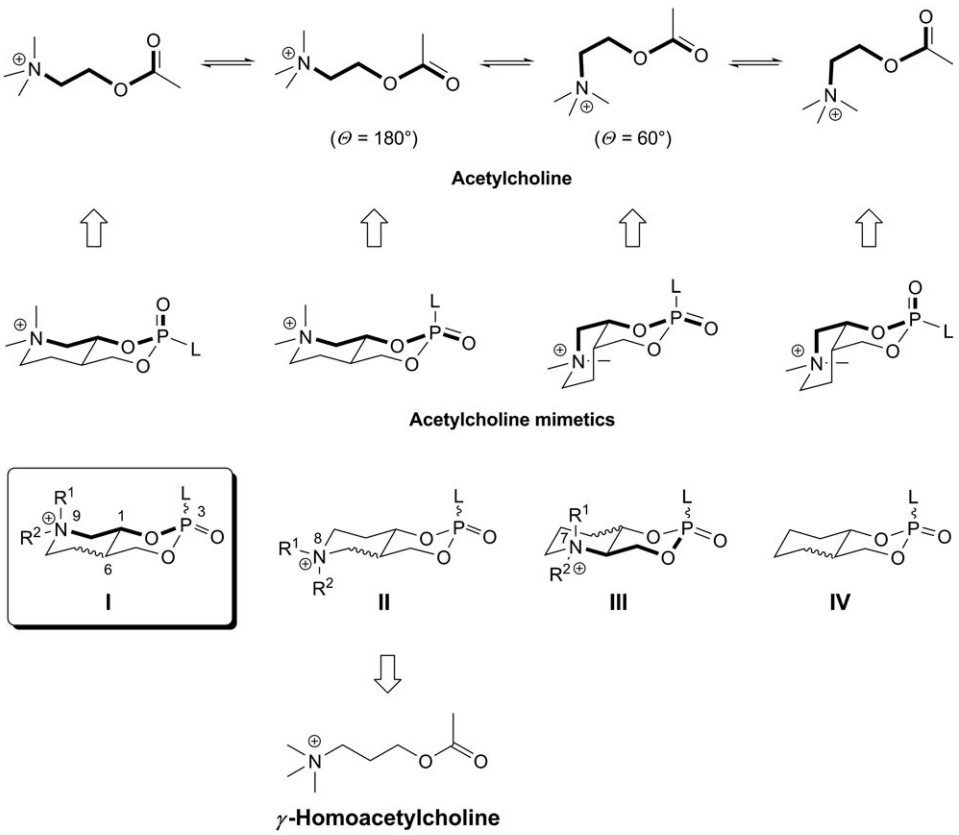

[a]) Structural types **I**–**IV**: *cis* and *trans*, and axially and equatorially P(3)-substituted isomers for each type
L = selected electron-withdrawing group, *e.g.*, F, Cl, 4-nitrophenoxy, 2,4-dinitrophenoxy, or amino acid derivatives (model compounds)
R^1, R^2 (tert. amines, free bases) = H, Me, CH_2Ph; R^1 = R^2 or $R^1 \neq R^2$

2. Synthesis and Characterization of the Precursors. – 2.1. *Ethyl (+)- and (−)-*trans-*and (+)- and (−)-*cis-*1-Benzyl-3-hydroxypiperidine-4-carboxylates* ((+)-**2** and (−)-**2** and (+)-**3** and (−)-**3**, resp.). 2.1.1. *General.* Reduction of ethyl 1-benzyl-3-oxopiperidine-4-carboxylate (**1**) with $NaBH_4$ gave the ethyl (±)-*trans*- and (±)-*cis*-1-benzyl-3-hydroxypiperidine-4-carboxylates ((±)-**2** and (±)-**3**, resp.; *Scheme 2*). The resulting four hydroxy esters could be separated directly by anal. HPLC on *Chiralcel® OD-H*

[1]) In [6], the discussion has been restricted to the characterization of the *cis*-hydroxy esters (+)- and (−)-**3** and its consequences in terms of a structural revision.

Scheme 2[a])

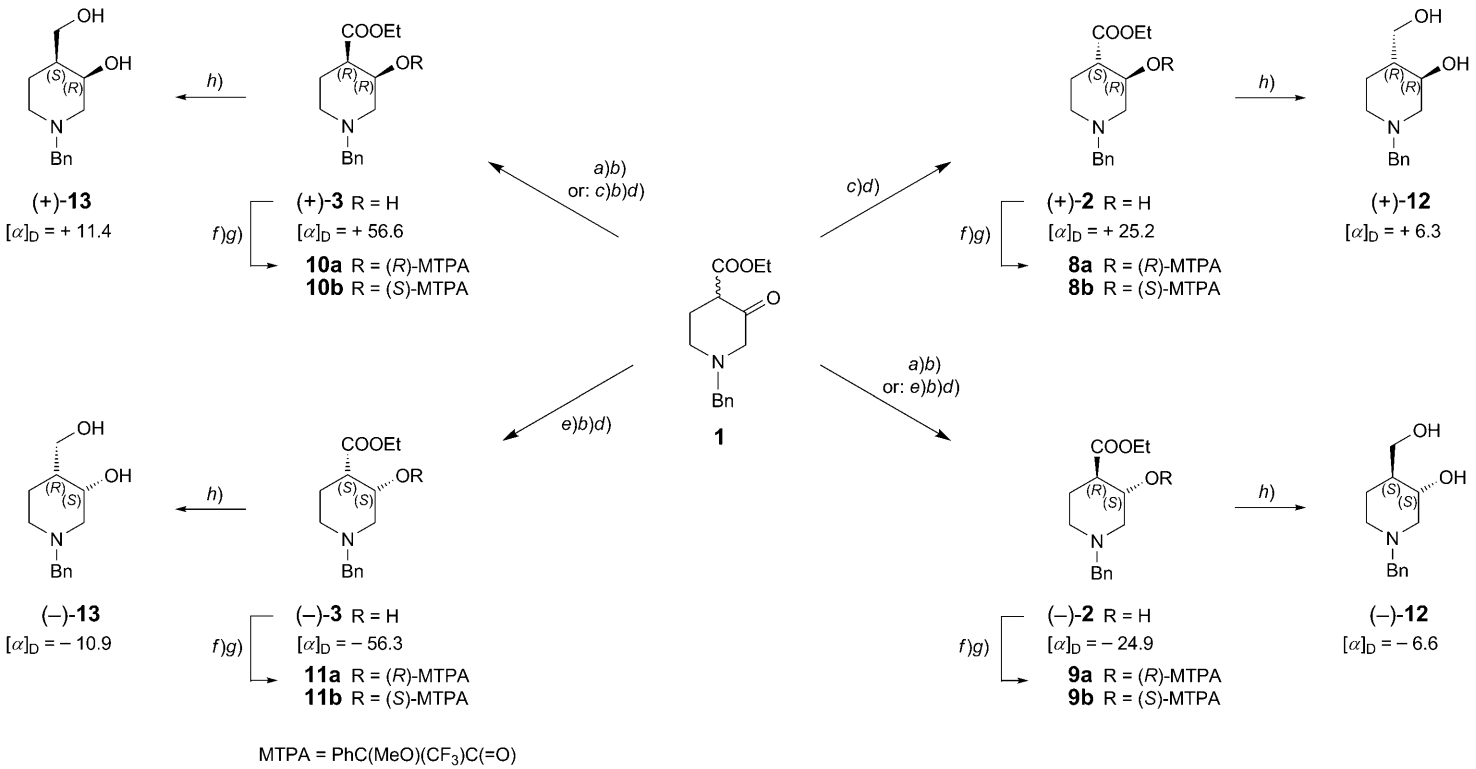

a) Bakers' yeast, H_2O, 30°. *b*) CC (SiO_2, CH_2Cl_2/MeOH). *c*) [Ru{(–)-(*S*)-binap}Cl(cym)]Cl, H_2, EtOH, 150°/100 bar. *d*) Prep. HPLC (*Chiralcel® OD*, hexane/EtOH). *e*) [Ru{(+)-(*R*)-binap}Cl(cym)]Cl, H_2, EtOH, 150°/100 bar. *f*) (–)-(*R*)- or (+)-(*S*)-MTPA-Cl, resp., pyridine, r.t. (note: (*R*)-MTPA-Cl yields the (*S*)-MTPA ester and *vice versa*). *g*) CC (SiO_2, CH_2Cl_2/MeOH). *h*) $LiAlH_4$, THF, CC (SiO_2, Et_2O).

[a]) $[\alpha]_D$ in $CHCl_3$ ($c = 1.00$), ee > 99%.

(*Fig. 1,a*; *Table 1*). Although the separation satisfied analytical purposes, the enantiomerically pure (+)- and (−)-*trans*- and (+)- and (−)-*cis*-3-hydroxy esters ((+)- and (−)-**2** and (+)- and (−)-**3**, resp.) were prepared more efficiently by enantioselective reductions (see below) [7].

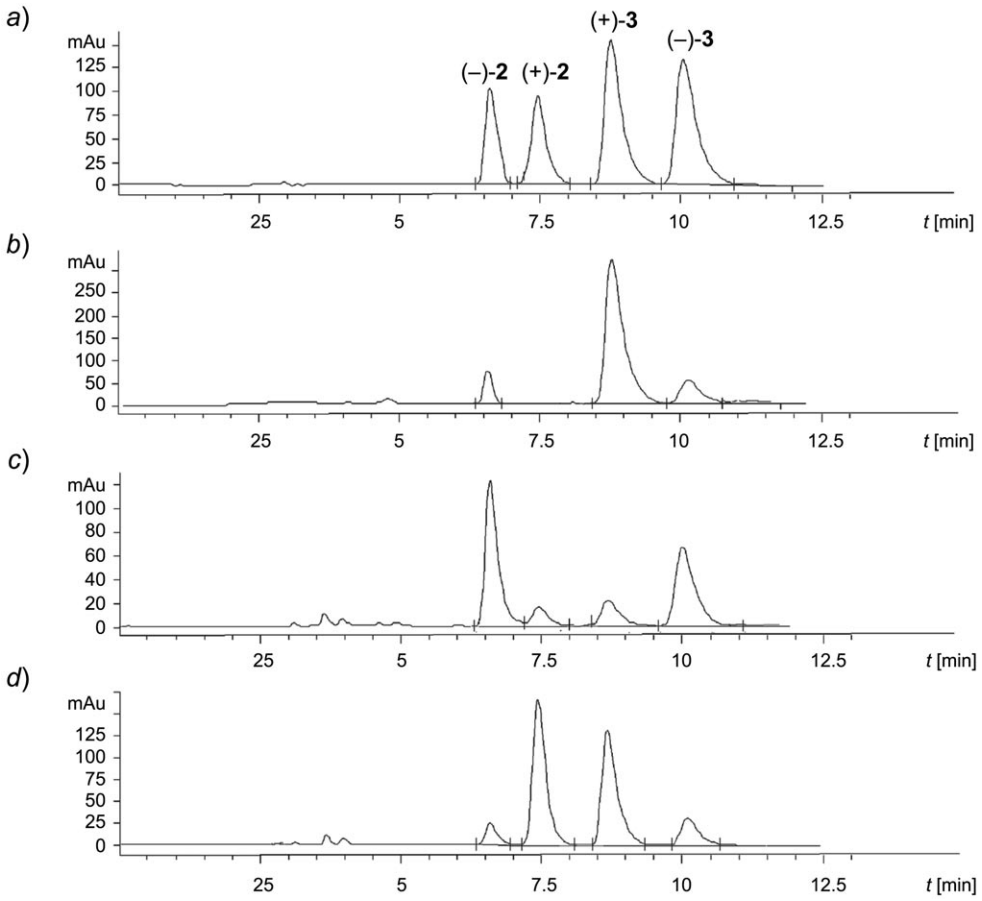

Fig. 1. *HPLC Traces* (*Chiralcel® OD-H* (5 μ), hexane/^{i}PrOH 12 : 1) *of the* trans- *and* cis-*ethyl 1-benzyl-3-hydroxypiperidine-4-carboxylates* **2** *and* **3**, *respectively, after reduction of ethyl 1-benzyl-3-oxopiperidine-4-carboxylate* (**1**) *under various conditions:* a) *$NaBH_4$*; b) *Bakers' yeast*; c) *[Ru{(+)-(R)-binap}Cl(cym)]Cl/H_2*; *d*) *[Ru{(−)-(S)-binap}Cl(cym)]Cl/H_2*

2.1.2. *Biological Reduction.* According to an established protocol [8], the piperidinone **1** was reduced with bakers' yeast under nonfermenting conditions to afford (−)-**2** (6%, $[\alpha]_D = -23.1$, ee 95%) and (+)-**3** (37%, $[\alpha]_D = +41.2$, ee 82%) after chromatography (SiO_2) [6].

2.1.3. *Stereoselective Hydrogenations.* To have access to all four stereoisomers of ethyl 1-benzyl-3-hydroxypiperidine-4-carboxylate, *i.e.*, to (+)- and (−)-**2** and (+)- and

Table 1. *Stereochemical Outcome of the Reduction of Ethyl 1-Benzyl-3-oxopiperidine-4-carboxylate* (**1**) *under Various Conditions: Anal. HPLC Parameters and Chiroptical Properties of the* trans- *and* cis-*Ethyl 1-Benzyl-3-hydroxypiperidine-4-carboxylates* **2** *and* **3**

Reducing agent	Product	k'[a])	ee [%][b])	$[\alpha]_D$[c])
$NaBH_4$	(±)-**2**	1.33, 1.71	–	–
	(±)-**3**	2.19, 2.75	–	–
Bakers' yeast	(−)-**2** ((3*S*,4*R*))	1.33	95	−23.1
	(+)-**3** ((3*R*,4*R*))	2.19	82	+41.2
[Ru{(+)-(*R*)-binap}Cl(cym)]Cl, H_2	(−)-**2** ((3*S*,4*R*))	1.33	67 (>99)[d])	−24.9[d])
	(−)-**3** ((3*S*,4*S*))	2.75	49 (>99)[d])	−56.3[d])
[Ru{(−)-(*S*)-binap}Cl(cym)]Cl, H_2	(+)-**2** ((3*R*,4*S*))	1.71	74 (>99)[d])	+25.2[d])
	(+)-**3** ((3*R*,4*R*))	2.19	41 (>99)[d])	+56.6[d])

[a]) k' = Retention factor; HPLC: *Chiralcel® OD-H* (5 μ, 250 × 4.6 mm), hexane/^{i}PrOH 12 : 1, flow-rate 1 ml/min, and $R_s > 2$. [b]) Determined according to area-%. [c]) $c = 1$, $CHCl_3$. [d]) After purification by preparative HPLC; *Chiralcel® OD* (10 μ, 250 × 20 mm), hexane/EtOH 15 : 1, flow-rate 5 ml/min, and $R_s > 2$.

(−)-**3**, the 3-oxo ester **1** was catalytically hydrogenated with both [Ru{(+)-(*R*)-binap}Cl(cym)]Cl and [Ru{(−)-(*S*)-binap}Cl(cym)]Cl (binap = [1,1′-binaphthalene]-2,2′-diylbis[diphenylphosphine], cym = *p*-cymene = 1-methyl-4-(1-methylethyl)benzene; see *Exper. Part*) according to [9] (*Scheme 2*, *Table 1*). Contrary to the biological reduction, the reactions proceeded with low diastereoselectivity (de *ca.* 10% in favor of the *cis*-isomers **3**, *Fig. 1*). Reaction with [Ru{(+)-(*R*)-binap}Cl(cym)]Cl and chromatographic separation (SiO_2) of the diastereoisomers yielded (−)-**2** (22%, ee 74%) and (−)-**3** (27%, ee 49%), and the analogous treatment with [Ru{(−)-(*S*)-binap}Cl-(cym)]Cl gave (+)-**2** (20%, ee 81%) and (+)-**3** (30%, ee 41%). Final chromatographic purification (*Chiralcel® OD*) afforded the enantiomerically pure 3-hydroxy esters (+)- and (−)-**2** and (+)- and (−)-**3** (*Scheme 1*, *Table 1*).

Although the hydrogenation conditions were optimized, the enantiofacial differentiation remained inefficient. This fact is explained by competitive directing effects [10] of the ester and the amine group present in **1**/**1′**[2]) that result in a set of coexistent equilibria and variably chelated species, *e.g.*, **A**, **A′**, **B**, and **B′** (*Scheme 3*). The assumption was verified when the benzyl group was replaced by electron-withdrawing substituents at the N-atom [7]. Catalytic hydrogenation of the derivatives **4**–**7** (*Scheme 3*) resulted in significantly increased ee values in the *cis* series, whereas those of the *trans* series remained almost unaffected. After exhaustive experimental studies, the highest enantioselectivity was observed with ethyl 1-(4-bromobenzoyl)-3-oxopiperidine-4-carboxylate (**7**)[3]): Hydrogenation of **7** in the presence of [Ru{(+)-(*R*)-binap}Cl(cym)]Cl yielded (−)-**2** (ee 66%) and (−)-**3** (ee 97%), and treatment with

---

[2]) According to the ^{1}H- and ^{13}C-NMR spectra, the enol form **1′** is predominant [7][11].

[3]) The tosyl (**4**), 4-nitrobenzoyl (**5**), and 2,4-dinitrobenzoyl (**6**) derivatives were less suited ($ee_{cis} < 75\%$, $ee_{trans} < 60\%$). Moreover, no satisfactory HPLC system for the separation of the corresponding resulting hydroxy esters could be elaborated, and the by-products due to the concomitant reduction of the SO_2 and NO_2 groups, respectively, could not be completely avoided. For details, see [7].

[Ru{(−)-(*S*)-binap}Cl(cym)]Cl gave (+)-**2** (ee 66%) and (+)-**3** (ee 83%) [7]. However, since all attempts to improve this still unsatisfactory result were not successful, the straightforward procedure with the 1-benzyl derivative **1** presented above was applied. In particular, the enantiomerically enriched fractions could be separated by prep. HPLC much more efficiently than the racemic mixtures.

Scheme 3[a])

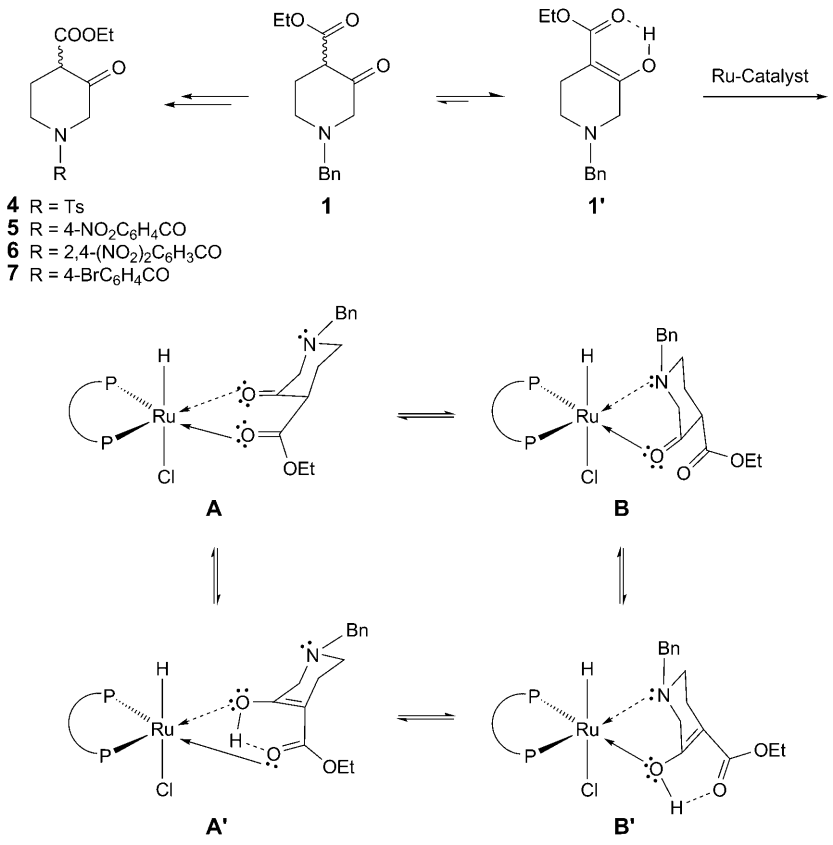

[a]) Selected arbitrary structures.

2.1.4. *Absolute Configurations.* As previously evidenced in detail [6], the (+)-(3*R*,4*R*)- and the (−)-(3*S*,4*S*)-configuration, respectively, were assigned to the *cis*-3-hydroxy esters (+)- and (−)-**3** by means of the high-field ^{1}H-NMR *Mosher* method [12] ((*R*)- and (*S*)-MTPA esters **10a**, **10b**, **11a**, and **11b**, in *Scheme 2*). Since the general applicability of this procedure to such piperidinols and -diols was confirmed [13][4]), the

[4]) It was not assured *a priori* that the *Mosher* method is reliably applicable to such N-heterocyclic compounds [6][13]. However, detailed differential analyses of the respective $\delta(S)-\delta(R)$ values allowed also assignments of the absolute configurations of bis-MTPA esters of hydroxypiperidinemethanols [13].

absolute configurations of the *trans*-3-hydroxy esters **2** could be established, too. Esterification of (+)- and (−)-**2** with (+)-(*S*)-MTPA-Cl (=(+)-(*S*)-α-methoxy-α-(trifluoromethyl)benzeneacetyl chloride) afforded the (*R*)-esters **8a** and **9a**, and the corresponding (*S*)-esters **8b** and **9b** were isolated after reaction of (+)- and (−)-**2** with (−)-(*R*)-MTPA-Cl (*Scheme 2*). From the $\delta(S)-\delta(R)$ values in the ^{1}H-NMR spectra of the **8a**/**9b** and the **9a**/**9b** couples, the (3*R*)-configuration for (+)-**2** and the (3*S*)-configuration for (−)-**2** could be unambiguously assigned (see *Exper. Part*).

These results confirm the stereochemical outcome of the biological reduction and fully corroborate the considerations on the [Ru^{II}(binap)]-catalyzed hydrogenations of related carbonyl compounds. The stereochemistry and the stereoselectivity of NAD(H)-dependent oxidoreductions are well investigated [14]. Bakers' yeast is a representative of E_3-type enzymes [15] that exhibit *pro*-(*R*)-H/*re*-face selectivity, and it shows pronounced *cis* diastereoselectivity in the reduction of cyclic ketones. Therefore, the main product of the biological reduction of the 3-oxopiperidine-4-carboxylate **1** is (3*R*,4*R*)-**3** as predicted [8][5]). The absolute configurations of the stereoisomeric 1-benzyl-3-hydroxypiperidine-4-carboxylates (+)- and (−)-**2** and (+)- and (−)-**3** (*Table 1*) are fully consistent with the empirically predicted face selectivity of the asymmetric H-transfer to functionalized ketones [9][17][18] and the dynamic kinetic resolution of 2-substituted 3-oxocarboxylic esters [18][19]. According to the very large number of experimental results, it can be concluded that [Ru{(−)-(*S*)(binap)}] has predominantly *si*-face and [Ru{(+)-(*R*)(binap)}] *re*-face selectivity, irrespective of the bulkiness and the character of the substituents that only affect the ee values.

2.2. *1-Benzyl-3-hydroxypiperidine-4-methanols* **12** *and* **13**. The enantiomerically pure diols, the *trans*-configured (+)-(3*R*,4*R*)- and (−)-(3*S*,4*S*)-1-benzyl-3-hydroxypiperidine-4-methanols ((+)-**12** and (−)-**12**, resp.) and the *cis*-configured (+)-(3*R*,4*S*)- and (−)-(3*S*,4*R*)-1-benzyl-3-hydroxypiperidine-4-methanols ((+)-**13** and (−)-**13**, resp.) were obtained after reduction of the corresponding ethyl 1-benzyl-3-hydroxypiperidine-4-carboxylates (+)- and (−)-**2** and (+)- and (−)-**3**, respectively, with $LiAlH_4$ (*Scheme 2*). The absolute configurations follow directly from their precursors.

3. Synthesis and Characterization of the 9-Benzyl-3-fluoro-2,4-dioxa-9-aza-3-phosphadecalins. – 3.1. *2,4-Dioxa-9-aza-phosphadecalins* **14** *and* **15**. The enantiomerically pure *trans*-9-benzyl-3-fluoro-2,4-dioxa-9-aza-3-phosphadecalin 3-oxides **14** (*Scheme 3*) were prepared from (+)- or (−)-**12** by reaction with $POCl_2F$ and chromatographic separation of the resulting *P(3)*-epimer mixture (axial/equatorial *ca.* 1:1) into the pure axial ((−)-**14a** and (+)-**14a**) and equatorial epimers ((−)-**14b** and (+)-**14b**)). Similarly, starting from (+)- or (−)-**13**, the *cis*-9-benzyl-3-fluoro-2,4-dioxa-9-aza-3-phosphadecalin 3-oxides ((+)-**15a** and (−)-**15a**, and (+)-**15b** and (−)-**15b**) were

---

[5]) The argumentation needs a remark: Although the definition of *re* and *si* is strictly based on the priority rules [16], it has been shown that rather the bulkiness and the hydrophobic characteristics of the carbonyl substituents determine the stereochemical course of biological reductions [14][15]. Hence, the synonyms R_L (large) and R_S (small) are more adequate. According to these considerations, C(4) is assigned as R_L and C(2) as R_S in **1** and the 'biological' *re*-face is accurately specified as *si*, see also [8].

obtained (*Scheme 4*). The NMR data of the 2,4-dioxa-9-aza-3-phosphadecalins **14** and **15** (see *Exper. Part*) exhibit the same essential features as the type-**IV** congeners (*Scheme 1*) [2–4]. In particular, the ^{31}P-NMR spectra confirm the relative configuration at the P-atom, the double-chair conformations of the axial epimers **14a** and **15a**, and distorted conformations [1–4][20] of the 2,4-dioxa-3-phospha moiety of the equatorial epimers (**14b** and **15b**)[6]). Due to the strongly electronegative F-substituent,

Scheme 4[a])

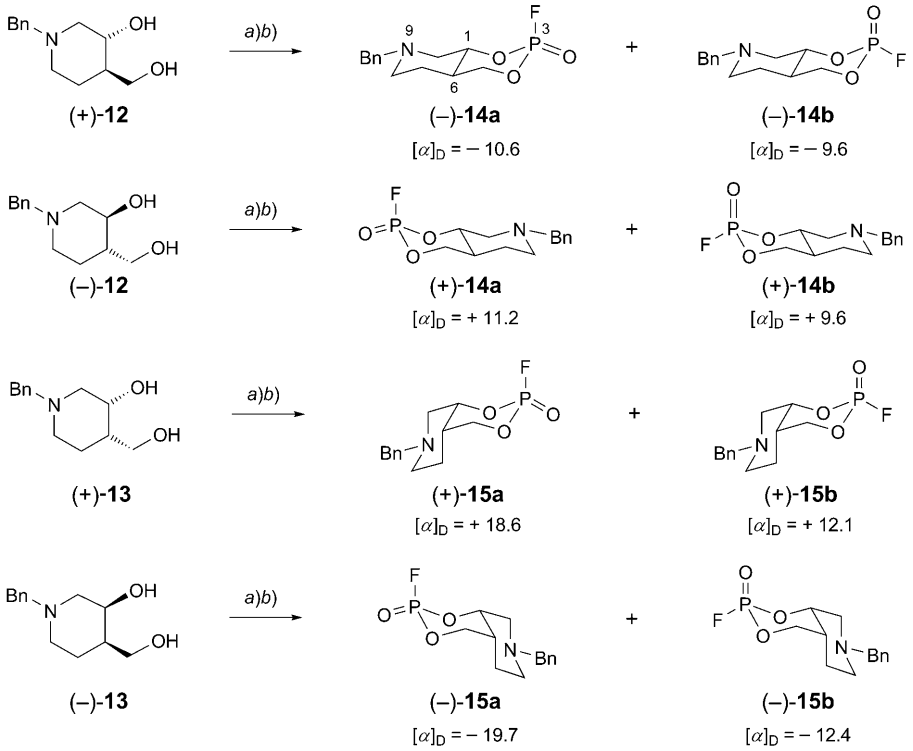

a) $P(O)Cl_2F$, pyridine, 0°. *b*) CC (SiO_2, hexane/Et_2O).

[a]) $[\alpha]_D$ in $CHCl_3$ ($c = 1.00$), ee > 99%.

---

[6]) Generally, the ^{31}P-NMR resonance of the axial epimer is shifted upfield with respect to the equatorial one, and the chemical-shift difference ($\Delta\delta = \delta_{eq} - \delta_{ax}$) is > 0, and its magnitude is inversely proportional to the electronegativity of the substituent at the P-atom. However, the cyclic phosphorofluoridates of the *cis*-series of the type **I**–**IV** compounds (*Scheme 1*, L = F) display $\Delta\delta < 0$, a fact that is only explained by significant conformational changes. The magnitude of the ^3J(P,H) in the ^{1}H-coupled ^{31}P-NMR is indicative of the conformation of the 2,4-dioxa-3-phospha moiety: Diagnostically relevant values for the axial epimers are $^3J(P,H_{eq}–C(5)) \approx 25$ Hz and $^3J(P,H_{ax}–C(5)) \approx 0$, whereas the equatorial ones display $^3J(P,H_{ax}–C(5)) \approx {}^3J(P,H_{eq}–C(5)) \approx 10$–15 Hz. Hence, the axial epimers exhibit a *d*-type and the equatorial ones a *m*-type splitting pattern (see [20]).

the chemical-shift difference ($\Delta\delta = \delta_{eq} - \delta_{ax}$) is small in the *trans*-couple **14a**/**14b** ($\Delta\delta = +0.6$ ppm) and even negative in the *cis*-couple **15a**/**15b** ($\Delta\delta = -0.4$ ppm).

3.2. *Conformations of* **14** *and* **15** *in Solution.* As discussed [1–4] and directly evidenced [20], the anomeric (stereoelectronic) effect is the predominant parameter that determines the conformation of the 3-substituted 2,4-dioxa-3-phosphadecalin 3-oxides[6]). In the 3-axially substituted 3-fluoro-3-phosphadecalins **14a** and **15a**, both the steric and the anomeric effects act in the same direction. As can be deduced from the ^{31}P-NMR chemical shifts and vicinal couplings (^3J(P,H))[6]), these compounds adopt the neat double-chair conformation (**C-1**)[7])[8]) (*Scheme 5*).

Scheme 5

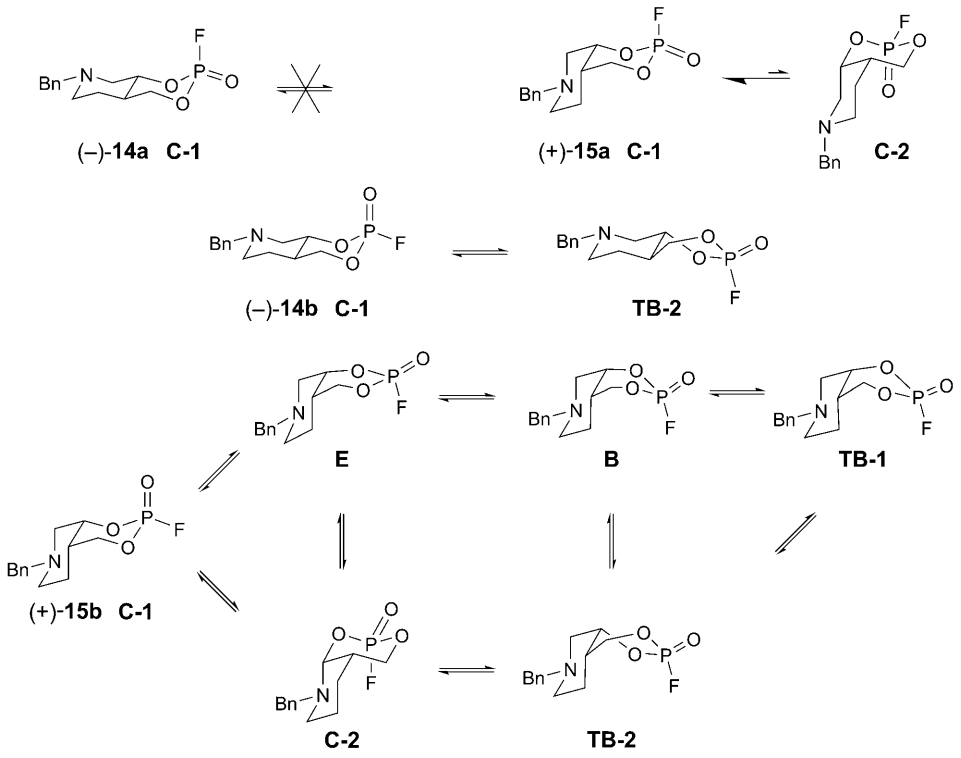

However, in the equatorial epimers **14b** and **15b**, the steric and the stereoelectronic effects are opposite. Although the chair conformation is sterically favored, the

[7]) The short terms for the conformations (IUPAC convention) were introduced in [20]: **C** = chair, **B** = boat, **E** = envelope, **TB** = twist-boat.

[8]) There is no direct evidence for the completely inverted **C-2** conformation. Hence, we assume that the strong anomeric preference prevents this interconversion.

anomeric preference of the F-substituent to move into an axial position results in nonchair conformations such as boat or twist-boats (*i.e.*, **B**, **TB-1**, and **TB-2**[7]); *Scheme 5*). According to the vicinal-coupling data (^3J(P,H–C(1)) ≈ 0, ^3J(P,H_{ax}–C(5)) = ^3J(P,H_{eq}–C(5)) = 10.5 Hz), and on the basis of our recent detailed conformational studies on the type-**III** [20–22] and type-**IV** congeners [21][22] (*Scheme 1*), we conclude by analogy that the *trans*-configured epimers **14b** exist in an equilibrium mixture of **C-1** and **TB-2** (*Scheme 5*)[9]).

The flexibility of the *cis*-decalin system and the *P(3)*-equatorial F-substituent render the situation significantly more complex, and additional conformations must be envisaged for the *cis*-configured equatorial epimers **15b**. In particular, the bicyclic system can undergo complete ring inversion to yield the prominent **C-2** arrangement (*Scheme 5*), which seems to be favored by the anomeric effect, the only drawback being the steric effect of the *N*-benzyl group[10]). With regard to the experimental ^3J(P,H–C(1)) = ^3J(P,H_{ax}–C(5)) = 16.5 Hz, and ^3J(P,H_{eq}–C(5)) = 7.5 Hz, none of the conformations depicted in *Scheme 5* can be excluded, nor can any be assigned. Hence, we assume that **15b** exists in solution as a complex mixture of **C-1**/**C-2**, and/or **TB-1**/**TB-2**, and most likely, also **B** and envelope **E** have to be considered[11]). A full account of our detailed conformational studies on the 3-fluoro-2,4-dioxa-3-phosphadecalin 3-oxides (types **I**–**IV**) will be presented later [22].

3.3. *Crystallographic Analysis of* (+)-**15a**[12]). The structure of (+)-**15a** was solved and refined successfully. The compound in the crystal was enantiomerically pure, and the absolute configuration of the molecule was determined independently by the diffraction experiment. The refinement of the absolute structure parameter (see *Exper. Part*) confidently confirmed that the refined coordinates (*Table 3*) represent the true enantiomorph with the expected (1*R*,3*S*,6*S*) configuration (*Fig. 2*). This result independently corroborates the configurational assignment of the precursor (+)-ethyl (3*R*,4*R*)-1-benzyl-3-hydroxypiperidine-4-carboxylate ((+)-**3**) by means of the high-field ^{1}H-NMR *Mosher* method and its reliability [6]. As discussed above, the six-membered ring containing the P-atom has an undistorted chair conformation with the F-atom in the axial position, and the *N*-benzyl group occupies the sterically favored equatorial position.

---

9) Since ^3J(P,H–C(1)) ≈ 0, conformations **B** and **TB-1** are excluded. The ^{31}P-NMR spectra are well resolved, and coalescence phenomena are not observed, *i.e.*, the interconversion **C-1** ⇌ **TB-2** is fast on the NMR time scale. In contrast to [20–22], the conformational assignments are tentative and not corroborated by variable-temperature NMR experiments nor X-ray crystallographic analyses.

10) According to crystal structures of 7-benzyl-3-fluoro-2,4-dioxa-7-aza-3-phosphadecalin 3-oxides (type **III**, *Scheme 1*) [20][21] and because of the lack of anomeric preferences, the piperidine moiety is assumed to adopt a chair conformation in solution with the *N*-benzyl group in an equatorial position; see also *Fig. 2*.

11) As discussed for **14b**, the conformational assignments are tentative, and the interconversions must be fast on the NMR time scale.

12) The full data set is summarized in *Table 3* (see *Exper. Part*). CCDC-802270 contains supplementary crystallographic data. These can be obtained free of charge from the *Cambridge Crystallographic Data Centre*, *via* www.ccdc.cam.ac.uk/data_request/cif.

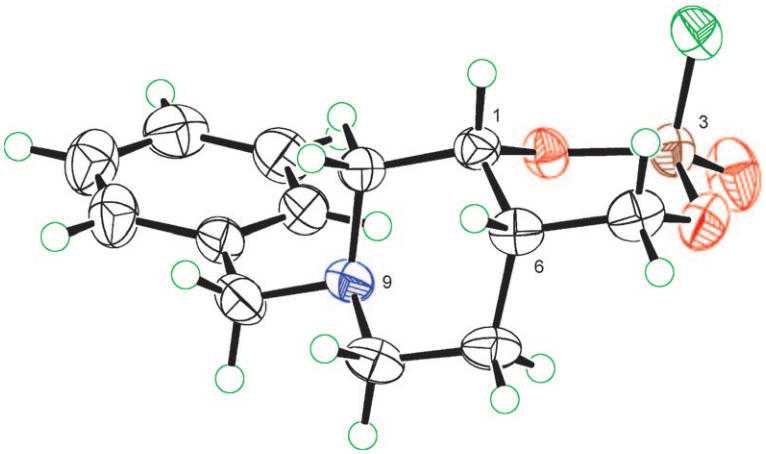

Fig. 2. *Molecular structure of (+)*-**15a** ((1*R*,3*S*,6*S*)). Trivial numbering; 50% probability ellipsoids.

4. Enzyme Kinetics. – 4.1. *General*. From the array of existing methods to evaluate kinetic data[13]), we rely in this report on the straightforward one according to [27]. In this approach, only the overall process is considered (*Scheme 6*), and the various imprecisions associated with such a simplified view are taken into account. Generally, the bimolecular rate constant (association constant k_a) is considered to be the most reliable parameter to indicate the inhibitory power of an organophosphate for an esterase. The most simple approach for evaluating k_a is based on the assumption that the inhibitor ***I*** and the esterase ***E*** react directly to form the irreversibly phosphorylated active center ***E*–*I*** (*Scheme 6*, mechanism *a*), and intermediate reactions are insignificant. A more detailed approach involves a preceding reversible step, resulting in the formation of an associative enzyme–inhibitor complex $\boldsymbol{E}\cdot\boldsymbol{I}^*$ followed by an irreversible phosphorylation step. The reversible step depends on the affinity of the inhibitor for the active site and is governed by the dissociation (or affinity) constant K_D, and the irreversible-phosphorylation constant k_p (*Scheme 6*, mechanism *b*). The latter parameters are related to the 'overall inhibitory potency' by the expression $k_i = k_p/K_D$, where k_i might be considered as a 'bimolecular reaction constant'. However, being a

---

[13]) Although apparently a simple theme, the reaction of an enzyme with a substrate and/or inhibitor to yield products or a modified (inhibited) enzyme species is a highly complex cycle with multiple equilibria and accordingly complex rate parameters. As a matter of fact, there exists no analytical solution for the exact description of the general case [23][24]. Hence, many procedures for data analyses are applied in the current literature, ranging from rather simplified ones [27] to highly sophisticated experimental and mathematical treatments, see, *e.g.*, [25]. However, being customized to the individual problems, none is generally applicable. Therefore, after a primary, still partial attempt [24], we have presented an integrated approach with a reappraisal of kinetic mechanisms and diagnostic methods [26]. In this context, first results with selected (+)- and (−)-3-fluoro-2,4-dioxa-3-phosphadecalin 3-oxides have been reported [2][21][26]. Because the kinetic experiments and the data evaluation for the (+)- and (−)-9-benzyl-3-fluoro-2,4-dioxa-9-aza-3-phosphadecalin 3-oxides **14** and **15** were performed earlier than the recent findings [26], the analysis of the assay data follows the procedure according to [24].

Scheme 6

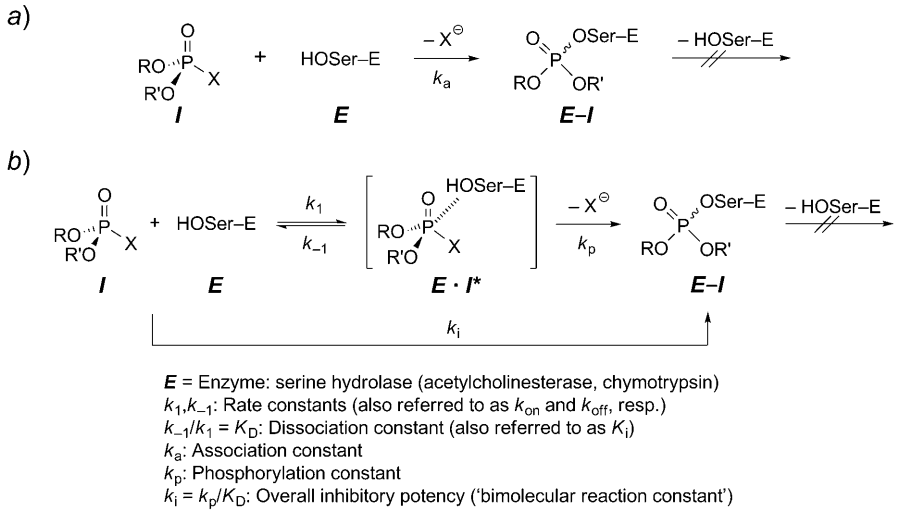

E = Enzyme: serine hydrolase (acetylcholinesterase, chymotrypsin)
k_1,k_{-1}: Rate constants (also referred to as k_{on} and k_{off}, resp.)
$k_{-1}/k_1 = K_D$: Dissociation constant (also referred to as K_i)
k_a: Association constant
k_p: Phosphorylation constant
$k_i = k_p/K_D$: Overall inhibitory potency ('bimolecular reaction constant')

combination of an equilibrium and a rate parameter, it is different from a real rate constant [27]. In particular, the treatment is applicable when the inhibition reaction follows first-order kinetics.

4.2. *Data Analysis and Results.* The inhibition studies were based on the *Ellman* assay [28]. The hydrolysis of the substrate acetylthiocholine (=2-(acetylthio)-*N*,*N*,*N*-trimethylethanaminium; ATC) was monitored photometrically at 412 ± 2 nm (liberation of the bis-anion of 5-mercapto-2-nitrobenzoic acid). Determination of the apparent rate constants k_{obs} from the progress curves and the mathematical evaluation of the dependence $k_{obs} = f([\boldsymbol{I}])$ to evaluate the inhibition parameters (K_D, k_a, k_i, and k_p) were performed according to [24]. The mathematical equations (*Eqns. 1–3*) underlying to *Scheme 6*, and further details are summarized in the *Exper. Part*. For all of the 8 stereoisomeric, enantiomerically pure (+)- and (−)-9-benzyl-3-fluoro-2,4-dioxa-9-aza-3-phosphadecalins **14** and **15**, the plot ($k_{obs} = f([\boldsymbol{I}])$) exhibited a linear dependence. Hence, they inhibited the enzyme irreversibly according to mechanism *a* that is only governed by the association constant (k_a)[14]). The experimental results are summarized in *Table 2*.

Table 2. *Kinetic Data of the Inhibition of AChE with the Enantiomerically Pure 9-Benzyl-3-fluoro-2,4-dioxa-9-aza-3-phosphadecalin 3-oxides (+)- and (−)-***14***, and (+)- and (−)-***15***.* P(O)F(^{i}Pr)$_2$ as reference.

	k_a [M^{-1}s^{-1}]	Mechanism		k_a [M^{-1}s^{-1}]	Mechanism
(+)-**14a**	12.1 ± 0.6	*a*	(+)-**15a**	8.6 ± 0.4	*a*
(−)-**14a**	23.8 ± 1.1	*a*	(−)-**15a**	8.2 ± 0.4	*a*
(+)-**14b**	10.7 ± 0.7	*a*	(+)-**15b**	7.6 ± 0.6	*a*
(−)-**14b**	14.2 ± 0.9	*a*	(−)-**15b**	8.4 ± 0.7	*a*
			P(O)F(O^{i}Pr)$_2$	242 ± 9	*a*

[14]) Mechanism *a* is equal to mechanism **1A** in the general approach [26].

Compared to diisopropyl phosphorofluoridate ($P(O)F(O^iPr)_2$) that is generally used as a very reliable standard reference, the type-**I** compounds are rather moderate inhibitors of AChE. They are significantly weaker than the type-**IV** congeners, and, in particular, do not display the pronounced diastereo- nor enantioselectivity as was observed with the latter [2][21][29]. The only exception is the couple (+)- and (−)-**14a** with the (3*S*)-configured (+)-**14a** being the most potent inhibitor of the type-**I** series[15]). Due to its *trans*-axial arrangement, we suggest that (+)-**14a** probably approximates a recognition conformation of ACh[16]). However, the rather scarce result does not show a consistent pattern allowing a reliable rationalization with respect to a structure–activity relationship[17]).

Remarks. – The hydrolysis of ACh catalyzed by AChE is a nearly diffusion-controlled, highly complex process, and all steps induce conformational changes of both the enzyme and the substrate. In view of this complexity, our reported experimental results do not allow reliable conclusions with respect to the effective inhibition mechanism (active site, peripheral or other conformatively induced irreversible binding at another nucleophilic site) of the investigated 9-benzyl-3-fluoro-2,4-dioxa-9-aza-3-phosphadecalin 3-oxides **14** and **15**. Although these compounds are regarded as the virtual ACh mimetics, their inhibitory power did not meet our expectations. Concerning the recognition conformation[18]), recent investigations [32] clearly indicate that no decisive conformation of a substrate (ACh or inhibitor) can be assigned without knowing the respective situation of the current state of the proceeding of the respective reaction. Moreover, as our compounds differ from the natural substrate and have additional structural features, in particular the *N*-benzyl group, that significantly could influence both the steric demand and the basicity of the compound, the situation is even more complicated, and conclusions of evidencing a recognition conformation from the inhibitory data is only speculative.

The authors are indebted to PD Dr. *A. Linden*, head of the X-ray department of our institute, for the high-quality X-ray crystallographic analysis. The financial support of the project by the *Swiss National Science Foundation* is gratefully acknowledged.

---

15) This result is consistent with the finding that the (S_P)-configuration seems to be preferred by serine hydrolases [30], and it agrees with our experience with the 8 stereoisomeric (+)- and (−)-3-fluoro-2,4-dioxa-3-phosphadecalin 3-oxides (type **IV**) [2][3][21][29].

16) It is fairly well established already by anterior work [31] that the most populated conformation of ACh is *gauche* with a torsion angle Θ between *ca.* 150 and 180° (*Scheme 1*).

17) Although the data were evaluated by the simplified method [24], they are considered to be reliable. Comparison of the data of the (+)- and (−)-3-fluoro-2,4-dioxa-3-phosphadecalin 3-oxides (type **IV**) that have been evaluated by either [24] and [26] did not exhibit fundamental differences, and the kinetic data were consistent on the whole [2][21][29]. However, the proceeding according to [26] enables subtle individual mechanistical refinements.

18) Many previous investigations suggest the existence of a physiologically active (recognition) conformation of ACh [31–35]. A comprehensive set of structural snapshots of the steps leading to the intermediates of catalysis and the potential regulation by substrate binding to various allosteric sites at the enzyme surface was presented recently [35]. It convincingly demonstrates that the ACh positioned in the active site adopts a relaxed *trans,gauche* conformation, consistent with the most stable conformation of ACh seen by crystallography [36] and NMR spectroscopy [37], whereas ACh bound in the peripheral anionic site adopts a nonrelaxed *trans,trans* conformation [35].

Experimental Part

1. *General*. See [1][4][6]. For the particular precautions in preparing and handling the organophosphates, see [1]. Enantioselective hydrogenations with {(+)-(1*R*)- and (−)-(1*S*)-[1,1′-binaphthalene]-2,2′-diylbis[diphenylphosphine-κP]}chloro[(1,2,3,4,5,6-η]-1-methyl-4-(1-methylethyl)benzene]ruthenium(1+) chloride ([Ru{(+)-(*R*)-binap}Cl(cym)]Cl and [Ru{(−)-(*S*)-binap}Cl(cym)]Cl, resp.; *Fluka 14800* and *14801*, resp.) were performed in a high-pressure reactor (*Parr 452 HC2*) equipped with a *Teflon*® vessel. The MTPA derivatives were prepared with (−)-(*R*)- and (+)-(*S*)-α-methoxy-α-(trifluoromethyl)benzeneacetyl chloride ((−)-(*R*)- and (+)-(*S*)-MTPA-Cl, resp.; *Fluka 65363* and *6536*, resp., *ChiraSelect*). CC = Column chromatography. Anal. HPLC: *Pharmacia-LKB* HPLC pump *2248*, *Hewlett-Packard-HP-1040M* diode-array detection system, data handling with a *Hewlett-Packard-HP-Chemstation* for LC, revision A.04.02; column *Chiralcel*® *OD-H* (5 μ, 250 × 4.6 mm; *Daicel Chemical Industries, Ltd.*); eluent hexane/^{i}PrOH 12 : 1; flow rate 1 ml/min at r.t.; λ_{det} 220 nm. Prep. HPLC: *Applied-Biosystems-400* solvent-delivery system, *Applied-Biosystems-783A* programmable absorbance detector; column *Chiralcel*® *OD* (10 μ, 250 × 20 mm); eluent hexane/EtOH 15 : 1; flow rate 5 ml/min at r.t.; λ_{det} 254 nm. Determination of ee: based on the integration of the peak areas of the anal. HPLC separations ($\alpha = 1.26$, $R_s > 2$). NMR Assignments: based on extensive 2D-NMR experiments (see [1]).

2. *Ethyl 3-hydroxy-1-(phenylmethyl)piperidine-4-carboxylates (+)- and (−)-***2** *and (+)- and (−)-***3**. 2.1. *(±)-Ethyl* trans- *and* cis*-3-Hydroxy-1-(phenylmethyl)piperidine-4-carboxylate (±)-***2** *and (±)-***3***, resp., and HPLC Separation of the Enantiomers.* To a soln. of ethyl 3-oxo-1-(phenylmethyl)piperidine-4-carboxylate hydrochloride (**1** · HCl; 551 mg, 1.85 mmol) and anh. Na_2CO_3 in anh. Et_2O (20 ml), $NaBH_4$ (49 mg, 1.28 mmol) was added in portions, and the mixture was stirred at r.t. for 1 h. Workup and continuous extraction with Et_2O yielded (±)-**2**/(±)-**3** as a yellowish oil (330 mg, 86%). Separation of the diastereoisomers was effected by CC (SiO_2, CH_2Cl_2/MeOH 98 : 2), but the four components of the mixture could be separated directly by anal. HPLC, too: (−)-**2** ($k' = 1.33$), (+)-**2** ($k' = 1.71$) ($\alpha = 1.29$, $R_S = 1.9$); (+)-**3** ($k' = 2.19$), (−)-**3** ($k' = 2.75$) ($\alpha = 1.26$, $R_S = 2.0$) (*Table 1*). Although the separation satisfied the anal. purposes, the enantiomerically pure compounds were prepared more efficiently by enantioselective hydrogenations, separation of the diastereoiomers, and final purification by prep. HPLC.

2.2. *(+)- and (−)-***2** (*trans* isomers) *and (+)- and (−)-***3** (*cis* isomers). The enantiomerically pure compounds were obtained as explicitly described in [6]: Bakers' yeast reduction of **1** afforded (−)-**2** ($[\alpha]_D = -23.1$, ee 95%) and (+)-**3** ($[\alpha]_D = +42.2$, ee 82%).

Hydrogenation of **1** with ([Ru{(−)-(*S*)-binap}Cl(cym)]Cl, gave (+)-**2** ($[\alpha]_D = +25.2$, ee > 99%) and (+)-**3** ($[\alpha]_D = +56.6$, ee > 99%). The analogous procedure with ([Ru{(+)-(*R*)-binap}Cl(cym)]Cl afforded (−)-**2** ($[\alpha]_D = -24.9$, ee > 99%) and (−)-**3** ($[\alpha]_D = -56.3$, ee > 99%).

*(+)-Ethyl (3*R*,4*S*)-3-Hydroxy-1-(phenylmethyl)piperidine-4-carboxylate* ((+)-**2**)*:* Colorless viscous oil. R_f (CH_2Cl_2/MeOH 98 : 2) 0.19. $[\alpha]_D = +25.2$ ($CHCl_3$, $c = 1.00$). IR (film): 3439*s*, 3086*m*, 3062*m*, 3028*s*, 2979*s* 2941v*s*, 2805*s*, 2765*s*, 1731v*s*, 1466*s*, 1453*s*, 1445*s*, 1395*s*, 1367*s*, 1320*s*, 1278v*s*, 1183v*s*, 1135*s*, 1089v*s*, 1037v*s*, 990*s*, 949*m*, 910*m*, 880*m*, 859*m*, 813*w*, 787*w*, 746v*s*, 700v*s*. ^{1}H-NMR (600 MHz, $CDCl_3$): 7.33 – 7.24 (*m*, *Ph*CH_2); 4.18 (*q*, $^3J = 7.1$, MeCH_2); 3.96 (*td*, $^3J(3,2ax) = {}^3J(3,4) = 9.1$, $^3J(3,2eq) = 4.2$, H–C(3)); 3.53, 3.525 (*AB*, $^2J = 13.2$, PhCH_2); 3.16 (br. *s*, OH); 2.99 (*ddd*, $^2J = 10.9$, $^3J(2eq,3) = 4.2$, $^4J(2eq,6eq) = 1.2$, H_{eq}–C(2)); 2.77 (*dtd*, $^2J = 11.2$, $^3J(6eq,5ax) = {}^3J(6eq,5eq) = 3.8$, $^4J(6eq,2eq) = 1.2$, H_{eq}–C(6)); 2.26 (*ddd*, $^3J(4,3) = 9.1$, $^3J(4,5ax) = 11.2$, $^3J(4,5eq) = 4.4$, H–C(4)); 2.06 (*td*, $^2J = {}^3J(6ax,5ax) = 11.1$, $^3J(6ax,5eq) = 2.9$, H_{ax}–C(6)); 2.04 – 1.95 (*m*, *dd*- and *dt*-like, $^2J \approx {}^3J \approx 11$, $^3J \approx 3$, H_{ax}–C(2), H_{eq}–C(5)); 1.73 (br. *qd*, $^2J \approx {}^3J(5ax,4) \approx {}^3J(5ax,6ax) \approx 11$, $^3J(5ax,6eq) \approx 3$, H_{ax}–C(5)); 1.27 (*t*, $^3J = 7.1$, *Me*CH_2). ^{13}C-NMR (75.4 MHz, $CDCl_3$): 174.2 (CO); 137.9 (C(1′)); 128.9 (C(3′), C(5′)); 128.2 (C(2′), C(6′)); 127.0 (C(4′)); 67.9 (C(3)); 62.5 (Ph*C*H_2); 60.6 (Me*C*H_2); 58.7 (C(2)); 52.1 (C(6)); 48.8 (C(4)); 26.4 (C(5)); 14.1 (*Me*CH_2). CI-MS (NH_3): 264 (100, $[M + H]^+$), 263 (12, M^+), 245 (15, $[M - H_2O]^+$).

*(−)-Ethyl (3*S*,4*R*)-3-Hydroxy-1-(phenylmethyl)piperidine-4-carboxylate* ((−)-**2**): $[\alpha]_D = -24.9$ ($CHCl_3$, $c = 1.00$). All other data: identical with those of (+)-**2**.

*(+)-Ethyl (3*R*,4*R*)-3-Hydroxy-1-(phenylmethyl)piperidine-4-carboxylate* ((+)-**3**): Colorless powder. M.p. *ca.* 35°. R_f (CH_2Cl_2/MeOH 98 : 2) 0.26. $[\alpha]_D = +56.6$ ($CHCl_3$, $c = 1.00$). All other data: see [6].

(−)-Ethyl (3S,4S)-3-Hydroxy-1-(phenylmethyl)piperidine-4-carboxylate ((−)-**3**): $[\alpha]_D = -56.3$ ($CHCl_3$, $c = 1.00$). All other data: identical with those of (+)-**3**, see [6].

3. *(R)- and (S)-MTPA Esters for the Determination of the Absolute Configuration*. The *trans*-3-hydroxy ester (+)- or (−)-**2** (40 mg, 0.15 mmol) was dissolved in dry pyridine (250 µl) and treated with (+)-(*S*)-MTPA-Cl (43 µl, 0.23 mmol, 1.5 equiv.) at r.t. for 24 h under Ar. Evaporation and chromatographic purification (SiO_2, CH_2Cl_2/MeOH 98 :2) of the crude product afforded the (*R*)-MTPA esters **8a** or **9a**, resp. Analogously, (+)- or (−)-**2**, resp., were treated with (−)-(*R*)-MTPA-Cl to yield the (*S*)-MTPA esters **8b** or **9b**, resp. All MTPA esters were isolated in pure form as colorless, viscous oils: **8a** (64 mg, 89%), **8b** (63 mg, 88%), **9a** (55 mg, 76%), and **9b** (58 mg, 81%).

*(R)- and (S)-MTPA Esters of (+)-**2**: Ethyl (3R,4S)-1-(phenylmethyl)-3-[(2R)-3,3,3-trifluoro-2-methoxy-1-oxo-2-phenylpropoxy]piperidine-4-carboxylate* ((*R*)-MTPA Ester; **8a**): ^{1}H-NMR (600 MHz, $CDCl_3$): 7.43 (*d*-like, $^3J = 8$), 7.31–7.17 (*m*, Ph); 5.37 (*td*, $^3J(3,2ax) = {}^3J(3,4) = 9.7$, $^3J(3,2eq) = 4.6$, H–C(3)); 3.93 (*q*, $^3J = 7.1$, MeCH_2); 3.56, 3.40 (*AB*, $^2J = 13.3$, PhCH_2); 3.43 (*d*, ^5J(Me,F) = 1.1, MeO); 3.15 (*ddd*, $^2J = 10.2$, $^3J(2eq,3) = 4.4$, $^4J(2eq,6eq) = 1.0$, H_{eq}–C(2)); 2.67 (br. *dt*, $^2J = 12.3$, $^3J(6eq,5ax) \approx {}^3J(6eq,5eq) \approx 4$, H_{eq}–C(6)); 2.46 (*ddd*, $^3J(4,3) = 9.7$, $^3J(4,5ax) = 11.3$, $^3J(4,5eq) = 4.7$, H–C(4)); 2.10 (*dd*, $^2J = 10.4$, $^3J(2ax,3) = 9.7$, H_{ax}–C(2)); 1.97 (*td*, $^2J = {}^3J(6ax,5ax) = 11.2$, $^3J(6ax,5eq) = 2.8$, H_{ax}–C(6)); 1.87 (br. *dq*, $^2J \approx 11$, $^3J(5eq,4) \approx {}^3J(5eq,6ax) \approx {}^3J(5eq,\ 6eq) \approx 4$, H_{eq}–C(5)); 1.72 (br. *qd*, $^2J \approx {}^3J(5ax,4) \approx {}^3J(5ax,6ax) \approx 11$, $^3J(5ax,6eq) \approx 4$, H_{ax}–C(5)); 1.07 (*t*, $^3J = 7.1$, *Me*CH_2). ^{13}C-NMR (75.4 MHz, $CDCl_3$): 172.4 (*C*OOEt); 165.4 (CO of MTPA); 137.3 (C(1′)); 132.1 (C(1″)); 129.4 (C(3′), C(5′)); 128.6 (C(3″), C(5″)); 128.1 (C(2′), C(6′), C(2″), C(6″)); 127.6 (C(4′)); 127.0 (C(4″)); 123.2 (*q*, ^1J(C,F) = 288.2, CF_3); 85.1 (*q*, ^2J(C,F) ≈ 40, Ph*C*(MeO)(CF_3)CO); 71.6 (C(3)); 62.4 (Ph*C*H_2); 60.8 (Me*C*H_2); 55.6 (MeO); 55.2 (C(2)); 51.8 (C(6)); 44.1 (C(4)); 22.8 (C(5)); 13.9 (*Me*CH_2). ^{19}F-NMR (564.5 MHz, $CDCl_3$): −72.21 (*s*, CF_3). CI-MS (NH_3): 497 (100, $[M + NH_4]^+$), 479 (13, M^+), 263 (12, $[M - \text{MTPA}]^+$), 245 (17, $[M + H - \text{MTPA} - H_2O]^+$).

Ethyl (3R,4S)-1-(Phenylmethyl)-3-[(2S)-3,3,3-trifluoro-2-methoxy-1-oxo-2-phenylpropoxy]piperidine-4-carboxylate ((*S*)-MTPA Ester; **8b**): ^{1}H-NMR (600 MHz, $CDCl_3$): 7.40 (*d*-like, $^3J = 7$), 7.39–7.15 (*m*, Ph); 5.37 (*td*, $^3J(3,2ax) = {}^3J(3,4) = 9.8$, $^3J(3,2eq) = 4.6$, H–C(3)); 4.03 (*q*, $^3J = 7.1$, MeCH_2); 3.53, 3.41 (*AB*, $^2J = 13.2$, PhCH_2); 3.42 (*d*, ^5J(Me,F) = 1.2, MeO); 3.11 (*ddd*, $^2J = 10.6$, $^3J(2eq,3) = 4.5$, $^4J(2eq,6eq) = 1.2$, H_{eq}–C(2)); 2.77 (br. *dt*, $^2J = 11.3$, $^3J(6eq,5ax) \approx {}^3J(6eq,5eq) \approx 3$, H_{eq}–C(6)); 2.46 (*ddd*, $^3J(4,3) = 9.8$, $^3J(4,5ax) = 11.8$, $^3J(4,5eq) = 4.5$, H–C(4)); 1.96–1.86 (*m*, H_{ax}–C(2), H_{eq}–C(5), H_{ax}–C(6)); 1.75 (br. *qd*, $^2J \approx {}^3J(5ax,4) \approx {}^3J(5ax,6ax) \approx 11$, $^3J(5ax,6eq) \approx 4$, H_{ax}–C(5)); 1.13 (*t*, $^3J = 7.1$, *Me*CH_2)). ^{13}C-NMR (75.4 MHz, $CDCl_3$): 172.4 (*C*OOEt); 165.4 (CO of MTPA); 137.3 (C(1′)); 132.1 (C(1″)); 129.5 (C(3′), C(5′)); 128.8 (C(3″), C(5″)); 128.2 (C(2′), C(6′), C(2″), C(6″)); 127.3 (C(4′)); 127.2 (C(4″)); 123.2 (*q*, ^1J(C,F) = 288.2, CF_3); 85.1 (*q*, ^2J(C,F) ≈ 40, Ph*C*(MeO)(CF_3)CO); 72.2 (C(3)); 62.1 (Ph*C*H_2); 60.8 (Me*C*H_2); 55.3 (MeO); 55.1 (C(2)); 51.2 (C(6)); 46.4 (C(4)); 27.4 (C(5)); 13.9 (*Me*CH_2). ^{19}F-NMR (564.5 MHz, $CDCl_3$): −72.07 (*s*, CF_3). CI-MS (NH_3): 497 (100, $[M + NH_4]^+$), 479 (15, M^+), 263 (9, $[M - \text{MTPA}]^+$), 245 (18, $[M + H - \text{MTPA} - H_2O]^+$).

$\Delta\delta(^1H) = \delta(S) - \delta(R)$ (in Hz)[19]): H–C(3) $\Delta\delta = 0$, H_{ax}–C(2) $\Delta\delta = -90$, H_{eq}–C(2) $\Delta\delta = -24$, MeCH_2 $\Delta\delta = +60$, and *Me*CH_2 $\Delta\delta = +36 \rightarrow$ (3*R*)-configuration. $\Delta\delta(^{19}F) = \delta(S) - \delta(R)$ (in Hz): CF_3 $\Delta\delta = +79 \rightarrow$ (3*R*)-configuration.

(R)- and (S)-MTPA Ester **9a** *and* **9b** *of* (−)-**2**. Being enantiomeric compounds, **9a** and **8b** (**9a** = *ent*-**8b**) as well as **9b** and **8a** (**9b** = *ent*-**8a**) exhibited identical NMR spectra, only the sign of the $\Delta\delta$ were inverted. $\Delta\delta(^1H) = \delta(S) - \delta(R)$ (in Hz)[19]): H–C(3) $\Delta\delta = 0$, H_{ax}–C(2) $\Delta\delta = +90$, H_{eq}–C(2) $\Delta\delta = +24$, MeCH_2, $\Delta\delta = -60$, and *Me*CH_2 $\Delta\delta = -36 \rightarrow$ (3*S*)-configuration. $\Delta\delta(^{19}F) = \delta(S) - \delta(R)$ (in Hz): CF_3 $\Delta\delta = -79 \rightarrow$ (3*S*)-configuration.

---

[19]) In contrast to the MTPA derivatives **10a**/**10b** and **11a**/**11b** of the *cis*-congeners (+)- and (−)-**3** [6], the ^{1}H-NMR signals were well resolved. For unambiguous additional comparisons, also MTPA esters starting from (±)-**2**, and from enantiomerically enriched (+)- and (−)-**2** (ee > 50%) were analyzed. The data of the respective diastereoisomer pairs were consistent in every respect and showed the relative displacements as expected [12]. Since **8a** = *ent*-**9b** and **8b** = *ent*-**9a**, **8a** (2′*R*,3*R*,4*S*) and **9b** (2′*S*,3*S*,4*R*) as well as **8b** (2′*S*,3*R*,4*S*) and **9a** (2′*R*,3*S*,4*R*) have identical NMR spectra.

The same procedure was adopted for the derivatization of the *cis*-3-hydroxy esters (+)- and (−)-**3** affording the (*R*)-MTPA esters **10a** and **11a**, resp., and the (*S*)-MTPA esters **10b** and **11b**, resp. For exper. details, the full data set, and the unambiguous assignment of the absolute configuration of the *cis*-3-hydroxy esters (+)- and (−)-**3**, see [6].

4. *3-Hydroxy-1-(phenylmethyl)piperidine-4-methanols (+)- and (−)-***12** (*trans* isomers) *and (+)- and (−)-***13** (*cis* isomers). To a cooled soln. (*ca.* 0°) of (+)- or (−)-**2** (350 mg, 1.33 mmol) in anh. THF (20 ml), $LiAlH_4$ (100 mg, 2.66 mmol) was slowly added in portions. After 30 min at 0°, the mixture was refluxed for 2 h. Continuous extraction with Et_2O, workup, and CC (SiO_2, Et_2O) afforded (+)-**12** (195 mg, 66%) or (−)-**12** (190 mg, 65%), resp. as colorless crystals. Analogously, the reduction of (+)- or (−)-**3** (400 mg, 1.52 mmol) afforded (+)-**13** (235 mg, 70%) or (−)-**13** (240 mg, 71%), resp.

*(+)-(3*R*,4*R*)-3-Hydroxy-1-(phenylmethyl)piperidine-4-methanol* ((+)-**12**): Colorless crystals. M.p. 111–112°. $[\alpha]_D = +6.3$ ($CHCl_3$, $c = 1.00$). All other data: identical with those of (±)-**12** as specified in [1].

*(−)-(3*S*,4*S*)-3-Hydroxy-1-(phenylmethyl)piperidine-4-methanol* ((−)-**12**): $[\alpha]_D = -6.6$ ($CHCl_3$, $c = 1.00$). All other data: identical with those of (+)-**12** (and (±)-**12** [1]).

*(+)-(3*R*,4*S*)-3-Hydroxy-1-(phenylmethyl)piperidine-4-methanol* ((+)-**13**). Colorless crystals. M.p. 82–84°. $[\alpha]_D = +11.4$ ($CHCl_3$, $c = 1.00$). All other data: identical with those of (±)-**13** as specified in [1].

*(−)-(3*S*,4*R*)-3-Hydroxy-1-(phenylmethyl)piperidine-4-methanol* ((−)-**13**). $[\alpha]_D = -10.9$ ($CHCl_3$, $c = 1.00$). All other data: identical with those of (+)-**13** (and (±)-**13** [1]).

5. trans- *and* cis-*9-Benzyl-3-fluoro-2,4-dioxa-9-aza-3-phosphadecalin 3-Oxides* (*=2-Fluorohexahydro-7-(phenylmethyl)-4*H*-1,3,2-dioxaphosphorino[4,5-*c*]pyridine 2-Oxides*) *(+)- and (−)-***14a**, *(+)- and (−)-***14b**, *(+)- and (−)-***15a**, *and (+)- and (−)-***15b**, *resp.* To a cooled soln. (0°) of (+)-**12** (113 mg, 0.87 mmol) in Et_2O (3 ml) in a glove box (N_2 atmosphere), anh. pyridine (125 µl (123 mg), 1.55 mmol) and a cooled soln. (0°) of $POCl_2F$ [38] (110 µl (173 mg), 1.26 mmol, *ca.* 1.5 equiv.) in Et_2O (1 ml) were added with a syringe, and the mixture was kept for *ca.* 2 min at 0° when the mixture was withdrawn and quickly passed through SiO_2 (pH 5.6 [4], Et_2O). The precipitated pyridinium salt in the reaction flask was thoroughly sonicated for 5 min with Et_2O, the combined solns. were gently evaporated (N_2 stream), and the residue was subjected to CC (SiO_2, pH 5.6 [4], hexane/Et_2O 4:1): (−)-**14a** (63 mg, 37%) and (−)-**14b** (63 mg, 37%).

Applying the identical procedure, the following compounds were prepared from the different starting diols (each 100 mg): from (−)-**12**, (+)-**14a** (54 mg, 36%) and (+)-**14b** (57 mg, 38%); from (+)-**13**, (+)-**15a** (51 mg, 34%) and (+)-**15b** (25 mg, 17%); from (−)-**13**, (−)-**15a** (71 mg, 47%) and (−)-**15b** (56 mg, 37%); in all cases the axial epimer was less polar.

*(+)-(1*S*,3*R*,6*S*)-9-Benzyl-3-fluoro-2,4-dioxa-9-aza-3-phosphadecalin 3-Oxide* (*=(+)-(2*R*,4a*S*,8a*S*)-2-Fluorohexahydro-7-(phenylmethyl)-4*H*-1,3,2-dioxaphosphorino[4,5-*c*]pyridine 2-Oxide*; (+)-**14a**): Colorless viscous oil. R_f (Et_2O) 0.18. $[\alpha]_D^{25} = +11.2$ ($c = 1.00$, $CHCl_3$). IR ($CHCl_3$): 2951*m*, 2928*m*, 2816*m*, 2774*m*, 1952*w*, 1877*w*, 1825*w*, 1602*w*, 1495*m*, 1468*m*, 1454*m*, 1444*m*, 1334*s*, 1306*m*, 1160*m*, 1070*s*, 1096*s*, 1072*s*, 1045*s*, 1009*s*, 982*s*, 933*m*, 899*s*, 882*s*, 858*m*. ^{1}H-NMR (600 MHz, $CDCl_3$): 7.27–7.19 (*m*, *Ph*CH_2); 4.30 (*A* of *ABX-P*, $^2J = 11.2$, ^3J(5eq,P) = 24.3, ^3J(5eq,6) = 4.4, H_{eq}–C(5)); 4.24 (*td*, $^3J(1,6) = {}^3J$(1,10ax) = 10.9, ^3J(1,10eq) = 4.2, H–C(1)); 4.10 (*B* of *ABX-P*, $^2J = {}^3J$(5ax,6) = 11.2, H_{ax}–C(5)); 3.53, 3.51 (*AB*, $^2J = 13.1$, PhCH_2); 3.11 (*ddd*, $^2J = 10.5$, ^3J(10eq,1) = 4.2, ^4J(10eq,8eq) = 1.5 (H_{eq}–C(10)); 2.85 (*dquint.*-like, $^2J = 11.5$, ^3J(8eq,7ax) ≈ ^3J(8eq,7eq) = 4.3, ^4J(8eq,10eq) = 1.5, H_{eq}–C(8)); 2.09 (*t*, $^2J = {}^3J$(10ax,1) = 10.5, H_{ax}–C(10)); 2.02 (*ddd*, $^2J = 11.5$, ^3J(8ax,7ax) = 12.4, ^3J(8ax,7eq) = 4.0, H_{ax}–C(8)); 1.92 (*X* of *ABX-P*, *qt*-like, $w_{1/2} \approx 25$, H–C(6)); 1.59 (*dq*, $^2J = 12.4$, ^3J(7eq,6) ≈ ^3J(7eq,8ax) ≈ ^3J(7eq,8eq) ≈ 4, H_{eq}–C(7)); 1.23 (*qd*, $^2J = {}^3J$(7ax,6) = ^3J(7ax,8ax) = 12.4, ^3J(7ax,8eq) = 4.3, H_{ax}–C(7)). ^{13}C-NMR (150.9 MHz, $CDCl_3$): 137.3 (C(1′)); 128.8 (C(3′), C(5′)); 128.3 (C(2′), C(6′)); 127.4 (C(4′)); 80.64 (*d*, ^2J(1,P) = 6.4, C(1)); 73.7 (*d*, ^2J(5,P) = 7.5, C(5)); 62.1 (PhCH_2); 56.6 (*d*, ^3J(10,P) = 11.9, C(10)); 51.7 (C(8)); 39.6 (*d*, ^3J(6,P) = 6.3, C(6)); 24.3 (C(7)). ^{31}P-NMR (121.4 MHz, $CDCl_3$): −16.5 (*dd*, ^1J(P,F) = 1008, ^3J(P,H_{eq}–C(5)) = 24.3). ^{19}F{^{1}H}-NMR (282.4 MHz, ($CDCl_3$): −86.1 (*d*, ^1J(F,P) = 1010). EI-MS: 285 (9, M^+), 194 (12, $[M - PhCH_2]^+$), 171 (21), 160 (26), 91 (100, $PhCH_2^+$), 65 (24).

*(−)-(1*R*,3*S*,6*R*)-9-Benzyl-3-fluoro-2,4-dioxa-9-aza-3-phosphadecalin 3-Oxide* ((−)-**14a**): $[\alpha]_D^{25} = -10.6$ ($c = 1.00$, $CHCl_3$). All other data: identical with those of (+)-**14a**.

*(+)-(1*S*,3*S*,6*S*)-9-Benzyl-3-fluoro-2,4-dioxa-9-aza-3-phosphadecalin 3-Oxide* (*(=2-Fluorohexahydro-7-(phenylmethyl)-4*H*-1,3,2-dioxaphosphorino[4,5-*c*]pyridine 2-Oxide* (+)-**14b**): Colorless prisms.

M.p. 88–92°. R_f (Et_2O) 0.09. $[\alpha]_D^{25} = +9.6$ ($c = 1.00$, $CHCl_3$). IR ($CHCl_3$): 2950*m*, 2930*m*, 2815*m*, 2773*m*, 1952*w*, 1878*w*, 1820*w*, 1711*w*, 1602*w*, 1494*m*, 1474*m*, 1468*m*, 1454*m*, 1332*s*, 1302*m*, 1159*m*, 1103*m*, 1053*s*, 1013*s*, 980*s*, 897*s*, 879*s*. ^{1}H-NMR (600 MHz, $CDCl_3$): 7.36–7.24 (*m*, *Ph*CH_2); 4.50–4.37 (*A* of *ABX-P* and *m*, not resolved, H_{eq}–C(5)[20]), H–C(1)); 4.21 (*B* of *ABX-P*, $^2J = {}^3J$(5ax,P) $= {}^3J$(5ax,6) $= 10.5$, ^4J(5ax,F) $= 4.0$, H_{ax}–C(5))[20]); 3.59, 3.585 (*AB*, $^2J = 13.2$, PhCH_2); 3.22 (*ddd*, $^2J = 10.6$, ^3J(10eq,1) $= 4.6$, ^4J(10eq,8eq) $= 1.5$, H_{eq}–C(10)); 2.91 (*dquint.*-like, $^2J = 11.6$, ^3J(8eq,7ax) $\approx {}^3J$(8eq,7eq) $= 4.0$, ^4J(8eq,10eq) $= 1.5$, H_{eq}–C(8)); 2.15 (*X* of *ABX-P*, *qt*-like, $w_{1/2} \approx 25$, H–C(6)); 2.13–2.03 (*m*, H_{ax}–C(8), H_{ax}–C(10)); 1.70 (*dq*, $^2J = 12.3$, ^3J(7eq,6) $\approx {}^3J$(7eq,8ax) $\approx {}^3J$(7eq,8eq) ≈ 4, H_{eq}–C(7)); 1.33 (*qd*, $^2J = {}^3J$(7ax,6) $= {}^3J$(7ax,8ax) $= 12.3$, ^3J(7ax,8eq) $= 4.3$, H_{ax}–C(7)). ^{13}C-NMR (150.9 MHz, $CDCl_3$): 137.1 (C(1′)); 128.8 (C(3′), C(5′)); 128.3 (C(2′), C(6′)), 127.4 (C(4′)); 80.2 (*d*, ^2J(1,P) $= 5.3$, C(1)); 73.6 (*d*, ^2J(5,P) $= 7.2$, C(5)); 62.0 (PhCH_2); 56.9 (*d*, ^3J(10,P) $= 8.9$, C(10)); 51.5 (C(8)); 38.4 (*d*, ^3J(6,P) $= 13.1$, C(6)); 24.3 (C(7)). ^{31}P-NMR (121.4 MHz, $CDCl_3$): -15.9 (*dt*, ^1J(P,F) $= 1002$, ^3J(P,H_{ax}–C(5)) $= {}^3J$(P,H_{eq}–C(5)) $= 10.5$)[20]). ^{19}F{^{1}H}-NMR (282.4 MHz, ($CDCl_3$): -69.4 (*d*, ^1J(F,P) $= 1000$). EI-MS: 285 (7, M^+), 194 (6, $[M - PhCH_2]^+$), 171 (15), 160 (18), 91 (100, $PhCH_2^+$), 65 (10).

*(−)-(1*R*,3*R*,6*R*)-9-Benzyl-3-fluoro-2,4-dioxa-9-aza-3-phosphadecalin 3-Oxide* ((−)-**14b**): $[\alpha]_D^{25} = -9.6$ ($c = 1.00$, $CHCl_3$). All other data: identical with those of (+)-**14b**.

*(+)-(1*R*,3*S*,6*S*)-9-Benzyl-3-fluoro-2,4-dioxa-9-aza-3-phosphadecalin 3-Oxide* (*= (+)-(2*S*,4a*S*,8a*R*)-2-Fluorohexahydro-7-(phenylmethyl)-4*H*-1,3,2-dioxaphosphorino[4,5-*c*]pyridine 2-Oxide*; (+)-**15a**): Colorless prisms. M.p. 75–77°. R_f (Et_2O) 0.13. $[\alpha]_D^{25} = +18.6$ ($c = 1.00$, $CHCl_3$). IR ($CHCl_3$): 2953*s*, 2812*s*, 2768*s*, 1955*w*, 1877*w*, 1816*w*, 1758*w*, 1601*w*, 1586*w*, 1495*m*, 1495*s*, 1454*s*, 1444*s*, 1371*s*, 1337*s*, 1272*s*, 1168*s*, 1125*s*, 1092*s*, 1075*s*, 1026*s*, 981*s*, 881*s*. ^{1}H-NMR (600 MHz, $CDCl_3$): 7.33–7.24 (*m*, *Ph*CH_2); 4.70 (*m*, $w_{1/2} \approx 6$, H–C(1)); 4.56 (*A* of *ABX-P*, $^2J = 11.4$, ^3J(5ax,P) $= 2.5$, ^3J(5ax,6ax) ≈ 0, H_{ax}–C(5))[20])[21]); 4.27 (*B* of *ABX-P*, $^2J = 11.4$, ^3J(5eq,P) $= 24.8$, ^3J(5eq,6) $= 1.2$, H_{eq}–C(5))[20]); 3.58, 3.55 (*AB*, $^2J = 13.5$, PhCH_2); 3.18 (*dt*, $^2J = 13.0$, ^3J(10eq,1) $= {}^4J$(10eq,8eq) $= 2.1$, H_{eq}–C(10)); 3.00 (*dquint.*-like, $^2J = 12$, ^3J(8eq,7ax) $\approx {}^3J$(8eq,7eq) ≈ 4.5, ^4J(8eq,10eq) $= 2.1$, H_{eq}–C(8)); 2.29 (*qd*, $^2J = {}^3J$(7ax,8ax) $= 12.0$, ^3J(7ax,8eq) $= 4.3$, H_{ax}–C(7)); 2.26 (*ddd*, $^2J = 13.0$, ^3J(10ax,1) $= 1.8$, ^4J(10ax,P) $= 5.9$, H_{ax}–C(10)); 2.12 (*td*, $^2J = {}^3J$(8ax,7ax) $= 11.7$, ^3J(8ax,7eq) $= 2.4$, H_{ax}–C(8)); 1.77 (*X* of *ABX-P*, *dquint.*-like, $w_{1/2} \approx 25$, H–C(6)); 1.56 (*m*, *dq*-like, $w_{1/2} \approx 25$, H_{eq}–C(7)). ^{13}C-NMR (150.9 MHz, $CDCl_3$): 137.5 (C(1′)); 128.7 (C(3′), C(5′)); 128.2 (C(2′), C(6′)); 127.1 (C(4′)); 78.5 (*d*, ^2J(1,P) $= 7.2$, C(1)); 73.1 (*d*, ^2J(5,P) $= 7.1$, C(5)); 61.9 (PhCH_2); 56.4 (*d*, ^3J(9,P) $= 9.1$, C(10)); 51.7 (C(8)); 34.3 (*d*, ^3J(6,P) $= 5.6$, C(6)); 22.8 (C(7)). ^{31}P-NMR (121.4 MHz, $CDCl_3$): -16.5 (*dd* br. *d*, ^1J(P,F) $= 1006$, ^3J(P,H_{eq}–C(5)) $= 24.8$, ^4J(P,H_{ax}–C(10)) $= 5.9$, ^3J(P,H_{ax}–C(6)) ≈ 2)[20]). ^{19}F{^{1}H}-NMR (282.4 MHz, ($CDCl_3$): -86.2 (*d*, ^1J(F,P) $= 1007$). EI-MS: 285 (16, M^+), 194 (5, $[M - PhCH_2]^+$), 160 (61), 147 (27), 118 (26), 91 (100, $PhCH_2^+$), 80 (27).

*(−)-(1*S*,3*R*,6*R*)-9-Benzyl-3-fluoro-2,4-dioxa-9-aza-3-phosphadecalin 3-Oxide* ((−)-**15a**): $[\alpha]_D^{25} = -19.7$ ($c = 1.00$, $CHCl_3$). All other data: identical with those of (+)-**15a**.

*(+)-(1*R*,3*R*,6*S*)-9-Benzyl-3-fluoro-2,4-dioxa-9-aza-3-phosphadecalin 3-Oxide* (*= (+)-(2*R*,4a*S*,8a*R*)-2-Fluorohexahydro-7-(phenylmethyl)-4*H*-1,3,2-dioxaphosphorino[4,5-*c*]pyridine 2-Oxide*; (+)-**15b**): Colorless plates. M.p. 95–98°. R_f (Et_2O) 0.07. $[\alpha]_D^{25} = +12.1$ ($c = 1.00$, $CHCl_3$). IR ($CHCl_3$): 2953*s*, 2930*s*, 2813*s*, 2787*s*, 2768*s*, 1954*w*, 1876*w*, 1816*w*, 1737*w*, 1602*w*, 1586*w*, 1495*m*, 1454*s*, 1443*s*, 1370*s*, 1329*s*, 1093*s*, 1076*s*, 1012*s*, 984*s*, 949*s*, 886*s*. ^{1}H-NMR (600 MHz, $CDCl_3$): 7.36–7.24 (*m*, *Ph*CH_2); 4.80 (*m*, not resolved, $w_{1/2} \approx 30$, H–C(1)); 4.53 (*A* of *ABX-P*, $^2J = 11.4$, ^3J(5ax,P) $= 16.5$, ^3J(5ax,6) $= 3.5$, H_{ax}–C(5))[20]); 4.39 (*B* of *ABX-P*, $^2J = 11.4$, ^3J(5eq,P) $= 16.5$, ^3J(5eq,6) $= 4.8$, H_{eq}–C(5))[20]); 3.58 (*s*, PhCH_2); 2.84 (*m*, *dt*-like, $^2J = 11.8$, H_{eq}–C(8)); 2.70 (*m*, *td*-like, $^2J = 11.8$, H_{eq}–C(8))); 2.44 (*m*, $w_{1/2} \approx 20$, CH_2(10)); 2.30 (*X* of *ABX-P*, *m*, $w_{1/2} \approx 30$, H–C(6)); 1.82 (*m*, *q*-like, $w_{1/2} \approx 15$, CH_2(7)). ^{13}C-NMR (150.9 MHz, $CDCl_3$): 137.2 (C(1′)); 128.7 (C(3′), C(5′)); 128.3 (C(2′), C(6′)); 127.3 (C(4′)); 79.2 (^2J(1,P) $= 7.7$, C(1)); 69.7 (*d*, ^2J(5,P) $= 6.4$, C(5)); 62.2 (PhCH_2); 53.6 (C(10)); 49.3 (C(8)); 32.8 (*d*, ^3J(6,P) $= 8.1$,

---

[20]) The descriptors 'ax' and 'eq' for CH_2(5) are based on their relative positions in the chair conformation of the 2,4-dioxa-3-phospha moiety. As discussed (see *Scheme 5*), the conformation is rather a twist-boat (**TB-2**) than a chair in the *P(3)*-equatorially substituted compounds. For reasons of simplicity, the notation 'ax' and 'eq' is maintained. H_{ax}–C(5) is alwayas *cis* to H–C(1) and H_{eq}–C(5) *trans* to H–C(1), see [20].

[21]) Assigned by ^{1}H{^{31}P} and ^{31}P/^{1}H-correlated spectra (HMQC).

C(6)); 24.3 (C(7)). ^{31}P-NMR (121.4 MHz, $CDCl_3$): −16.9 (*dtd*, $^1J(P,F) = 997$, $^3J(P,H–C(1)) = {}^3J(P,H_{ax}–C(5)) = 16.5$, $^3J(P,H_{eq}–C(5)) = 7.5$)[20]. ^{19}F{^{1}H}-NMR (282.4 MHz, ($CDCl_3$): −76.9 (*d*, $^1J(F,P) = 999$). EI-MS: 285 (16, M^+), 194 (24, $[M - PhCH_2]^+$), 160 (51), 147 (19), 118 (23), 91 (100, $PhCH_2^+$), 80 (32).

*(−)-(1*S*,3*S*,6*R*)-9-Benzyl-3-fluoro-2,4-dioxa-9-aza-3-phosphadecalin 3-Oxide* ((−)-**15b**): $[\alpha]_D^{25} = -12.4$ ($c = 1.00$, $CHCl_3$). All other data: identical with those of (+)-**15b**.

*5. X-Ray Crystal-Structure Determination of (+)-***15a**[12]). All measurements were conducted at low-temperature by means of a *Nonius-KappaCCD* area-detector diffractometer [39] with graphite-monochromated MoK_α radiation (λ 0.71073 Å) and an *Oxford-Cryosystems-Cryostream-700* cooler. The unit-cell constants and an orientation matrix for data collection were obtained from a least-squares refinement of the setting angles of 28171 reflections in the range $4° < 2\theta < 50°$. The mosaicity was 1.033(2)°. A total of 222 frames were collected by using ω scans with κ offsets, 100-s exposure time, a rotation angle of 2.0° per frame, and a crystal-detector distance of 30.0 mm.

Data reduction was performed with HKL DENZO and SCALEPACK [40]. The intensities were corrected for *Lorentz* and polarization effects, and an absorption correction based on the multi-scan method [41] was applied. The space group was determined from the systematic absences, packing considerations, a statistical analysis of intensity distribution, and the successful solution and refinement of the structure. Equivalent reflections, other than *Friedel* pairs, were merged. Data collection and refinement parameters are compiled in *Table 3*. A view of the molecule is depicted in *Fig. 2*.

The structure was solved by direct methods with SIR92 [42], which revealed the positions of all non-H-atoms. There are two symmetry-independent molecules in the asymmetric unit. Both have the same configuration and very similar conformations. The atomic coordinates of the two molecules were tested carefully for a relationship from a higher-symmetry space group with the program PLATON [43], but none could be found. The non-H-atoms were refined anisotropically. All of the H-atoms were placed in geometrically calculated positions and refined with a riding model where each H-atom was assigned a fixed isotropic displacement parameter with a value equal to $1.2U_{eq}$ of its parent atom. Refinement of the structure was carried out on F^2 by using full-matrix least-squares procedures, which minimized the function $\Sigma w(F_o^2 - F_c^2)^2$. The weighting scheme was based on counting statistics and included a factor to downweight the intense reflections. Plots of $\Sigma w(F_o^2 - F_c^2)^2$ *vs.* F/F_c(max) and resolution showed no unusual trends. A correction for secondary extinction was applied. Refinement of the absolute structure parameter [44] yielded a value of 0.04(8), which confidently confirms that the refined coordinates, as listed in *Table 3*, represent the true enantiomorph. Neutral-atom-scattering factors for non-H-atoms were taken from [45], and the scattering factors for H-atoms were taken from [46]. Anomalous dispersion effects were included in F_c [47]; the values for f' and f'' were those of [48]. The values of the mass attenuation coefficients were those of [49]. All calculations were performed with the SHELXL97 program [50], and the crystallographic diagram was drawn with ORTEPII [51].

6. *Enzyme Kinetics.* 6.1. *General.* Acetylcholinesterase (AChE) from *Electrophorus electricus* (electric eel), *Sigma C-2888*, type V-S, lyophilized powder ≥1000 units/mg protein; acetylthiocholine (ATC), *Fluka 01480 BioChemika*; 5,5′-dithiobis[2-nitrobenzoic acid] (DTNB, *Ellmans* reagent [28]), *Fluka 43760 BioChemika*; diisopropyl fluorophosphate (=diisopropyl phosphorofluoridate; DFP), *Fluka 38399 purum*; H_2O, *Fluka*, *95304* (HPLC quality); MeCN, *Fluka 00695 puriss.*, abs. (over molecular sieves); NaCl, *Fluka 71378 BioChemika MicroSelect*; $NaH_2PO_4 \cdot H_2O$, *Merck 6346 p.a.*; $Na_2HPO_4 \cdot 2\,H_2O$, *Merck 6580 p.a.*; *Pluronic F-68, Sigma P-1300* (lot 88 H1000); *Tris* buffer, *Fluka 93349 BioChemika MicroSelect*. Volumes ≤1 ml were measured accurately with microliter pipettes *Socorex S+* (100–1000 µl) and *Socorex Autoclavable Calibra 822* (10–100 µl, 1–10 µl), volumes <1 ml by diluting in volumetric flasks. pH Determinations: *Knick Portamess 762 Calimatic*; electrode, *Mettler InLab 423 S7*; calibration, *Mettler* standard buffers pH 4.01 and pH 7.00; electrolyte, *Mettler* standard, 3M KCl sat. with AgCl; measurements at 22°, accuracy ± 0.02 pH units. Enzyme kinetic progress curves and photometric titration of the active sites of AChE: *Hewlett-Packard-8452A* diode-array spectrophotometer with *HP 89532A* UV-VIS software (revision A.00.00). Curve fitting and data analyses were performed with *OriginPro 7.5G SR3 v.7.5853* (www.originlab.com).

6.2. *Phosphate Buffer pH 7.00.* Soln. A: $Na_2HPO_4 \cdot 2\,H_2O$ (4.45 g), NaCl (1.46 g), and *Pluronic F-68* (25 mg) were dissolved in H_2O (250 ml). Soln. B: $NaH_2PO_4 \cdot H_2O$ (6.90 g), NaCl (2.92 g), and *Pluronic*

Table 3. *Crystallographic Data* of *(+)*-**15a**

Crystallized from	hexane/acetone	$2\theta_{max}$ [°]	50
Empirical formula	$C_{13}H_{17}FNO_3P$	Transmission factors	0.788; 0.985
M_r	285.25	(min; max)	
Crystal color, habit	colorless, prism	Total reflections	20334
Crystal dimensions	$0.10 \times 0.15 \times 0.28$	measured	
[mm]		Symmetry-independent	4866
Temperature [K]	160(1)	reflections	
Crystal system	monoclinic	R_{int}	0.068
Space group	$P2_1$ (#4)	Reflections with $I > 2\sigma(I)$	4201
Z	4	Reflections used in	4866
Reflections for	28171	refinement	
cell determination		Parameters refined;	345; 1
2θ Range for	4 – 50	restraints	
cell determination [°]		Final $R(F)$ ($I > 2\sigma(I)$	0.0361
Unit cell parameters:		reflections)	
a[Å]	6.3402(3)	$wR(F^2)$ (all data)	0.0887
b[Å]	4.6194(7)	Weights	$w = [\sigma^2(F_o^2) + (0.0431P)^2 + 0.1989P]^{-1}$
c[Å]	15.0597(6)		where $P = (F_o^2 + 2F_c^2)/3$
β[°]	98.441(2)	Goodness of fit	1.047
V [Å^3]	1380.8(1)	Secondary extinction	0.015(2)
$F(000)$	600	coefficient	
D_x [g cm^{-3}]	1.372	Final Δ_{max}/σ	0.001
μ(MoK_α) [mm^{-1}]	0.214	$\Delta\rho$ (max; min) [e Å^{-3}]	0.17; −0.20
Scan type	ω	$\sigma(d_{(C-C)})$ [Å]	0.003 – 0.005

F-68 (25 mg) were dissolved in H_2O (500 ml). The solns. were adjusted to pH 7.00 ± 0.02 by mixing. Prior to use, the buffer was filtered (*TRP* syringe filter, max. 0.5 MPa, PES-membrane 0.22 µ, gamma-sterilized, free of pyrogens).

6.3. *AChE Solution.* AChE (1 mg) was dissolved in the phosphate buffer pH 7.00 (1 ml), thoroughly mixed, and stored at 5° (stock soln.). To the phosphate buffer (5 ml), AChE stock soln. (5 µl) was added and thoroughly mixed. The soln. (1 ml) was diluted to 10 ml with phosphate buffer. Such a soln. could be used for the determination of K_m and one assay series.

6.4. *ATC and DTNB Solutions.* ATC (22.6 mg) was dissolved in phosphate buffer (1 ml; → 78 mM) and thoroughly mixed. The soln. was freshly prepared prior to use and stored at 0° (ice bath). DTNB (15 mg) was dissolved in phosphate buffer (2 ml; → 19 mM) and well mixed prior to use.

6.5. *Inhibitor Solution* (representative example). The respective 3-substituted 3-phosphadecalin (3.5 mg) was dissolved in abs. MeCN (200 µl). From this stock soln., a dilution series was prepared to yield five different concentrations. The total volume of each assay was 25 µl.

6.6. *Determination of* K_m. Prior to each assay series, the *Michaelis* constant (K_m) was determined under the assay conditions (instead of an inhibitor, MeCN (25 µl) was added). The linear increase of the absorption was monitored at 412 ± 2 nm at five different concentrations of the substrate (ATC) ([S] = [ATC] from 100 – 500 µM). The k_{obs} values were treated according to zeroth-order kinetics (v = constant). K_m was calculated from the resulting straight line of the plot $1/k_{obs} = f(1/[S])$; K_m was always in the range of 160 µM.

6.7. Ellman-*Assay* [28]. In a polystyrene cell (4 ml, $d = 1$ cm), phosphate buffer pH 7.00 (2 ml), DTNB soln. (100 µl), and ATC soln. (20 µl) were mixed and thermostatted at 25°. Then inhibitor soln. (x µl, known [***I***], $x \leq 25$ µl), and MeCN ((25 − x) µl) were added. At $t = 0$, the AChE soln. (1 ml) was added and the mixture gently mixed for 5 s. After 10 s, the monitoring of the absorption at 412 ± 2 nm (liberated bis-anion of 5-mercapto-2-nitrobenzoic acid) automatically started, and 600 data points were collected

for 10 min at various concentrations of the inhibitor. As in the K_m determinations, the total volume was 3.15 µl and the concentration of the substrate [S] = 497 µM. Per inhibitor, at least five measurements with different inhibitor concentrations were performed, the smallest one being *ca.* 1/5 – 1/10 of the largest one. The largest concentration sufficient for the determination of $P(O)F(O^iPr)_2$ (DFP) was *ca.* 160 µM.

6.8. *Data Analysis* [24]. The integrated rate equation describing product generation (monitored by the absorbance A) and the apparent rate constants k_{obs} is given by *Eqn. 1*. It is fitted ($R > 0.999$) to progress curves recorded at fixed [S] and variable [***I***] (primary plot, $A = f(t)$) to obtain a series of k_{obs} values and their standard errors (SE). The inhibition parameters are obtained from the secondary plots ($k_{obs} = f([\boldsymbol{I}])$) that result from weighted (SE^{-2}) linear or nonlinear regression according to *Eqns. 2* or *3*. The analysis of these plots enables a differentiation between the inhibition mechanisms: k_{obs} depends linearly upon the inhibitor concentration for mechanism *a* and hyperbolically for mechanism *b*. For mechanism *a*, the k_a values are calculated according to *Eqn. 2*, its slope $k_{obs}/[\boldsymbol{I}]$ is obtained from the linear regression. The decisive plot for mechanism *b* is doubly reciprocal ($1/k_{obs} = f(1/[\boldsymbol{I}])$, *Eqn. 3*), and the K_D and k_p values are calculated by linear regression, the slope being $(K_D/k_p)(1 + [S]/K_m)$ and the intercept $1/k_p$. The overall inhibitory potency k_i is expressed by k_p/K_D (see *Scheme 6*).

$$A = \frac{v_z}{k_{obs}}\left(1 - e^{-k_{obs}\cdot t}\right) \tag{1}$$

$$k_a = \left(\frac{k_{obs}}{[I]}\right)\left(1 + \frac{[S]}{K_m}\right) \tag{2}$$

$$\frac{1}{k_{obs}} = \left(\frac{K_D}{k_p}\right)\left(1 + \frac{[S]}{K_m}\right)\left(\frac{1}{[I]}\right) - \frac{1}{k_p} \tag{3}$$

a) $\boldsymbol{I} + \boldsymbol{E} \xrightarrow{k_a} \boldsymbol{E}\text{–}\boldsymbol{I}$

b) $\boldsymbol{I} + \boldsymbol{E} \overset{K_D}{\rightleftharpoons} [\boldsymbol{E}\cdot\boldsymbol{I}^*] \xrightarrow{k_p} \boldsymbol{E}\text{–}\boldsymbol{I}$, with k_i connecting $\boldsymbol{I}$ and $\boldsymbol{E}\text{–}\boldsymbol{I}$

6.9. *Results.* For all eight stereoisomeric 3-fluoro-2,4-dioxa-9-aza-3-phosphadecalinoxides **14** and **15**, the secondary plot ($k_{obs} = f([\boldsymbol{I}])$) exhibited a linear dependence. This behavior indicates that the inhibition follows mechanism *a* for all compounds.

REFERENCES

[1] S. Furegati, W. Ganci, F. Gorla, U. Ringeisen, P. Rüedi, *Helv. Chim. Acta* **2004**, *87*, 2629.
[2] M. Wächter, P. Rüedi, *Chem. Biodiversity* **2009**, *6*, 283.
[3] W. Ganci, E. J. M. Meier, F. Merckling, G. Przibille, U. Ringeisen, P. Rüedi, *Helv. Chim. Acta* **1997**, *80*, 421; S. Furegati, W. Ganci, G. Przibille, P. Rüedi, *Helv. Chim. Acta* **1998**, *81*, 1127.
[4] M. J. Stöckli, P. Rüedi, *Helv. Chim. Acta* **2001**, *84*, 106; M. J. Stöckli, P. Rüedi, *Helv. Chim. Acta* **2007**, *90*, 2058.
[5] S. Furegati, F. Gorla, A. Linden, P. Rüedi, *Chem.-Biol. Interact.* **2005**, *157–158*, 415.
[6] P. A. Lorenzetto, A. Strehler, P. Rüedi, *Helv. Chim. Acta* **2006**, *89*, 3023.
[7] P. G. Lorenzetto, 'Synthese und Charakterisierung der enantiomerenreinen 9-Aza-3-phosphadecaline als Acetylcholin-Mimetika', Ph.D. Thesis, University of Zurich, 2009.
[8] D. Seebach, S. Roggo, T. Maetzke, H. Braunschweiger, J. Cercus, M. Krieger, *Helv. Chim. Acta* **1987**, *70*, 1605.
[9] R. Noyori, T. Ohkuma, M. Kitamura, H. Takaya, N. Sayo, H. Kumobayashi, S. Akutagawa, *J. Am. Chem. Soc.* **1987**, *109*, 5856; M. Kitamura, M. Tokunaga, T. Ohkuma, R. Noyori, *Org. Synth.* **1993**, *71*, 1.

[10] M. Kitamura, T. Ohkuma, S. Inoue, N. Sayo, H. Kumobayashi, S. Akutagawa, T. Ohta, H. Takaya, R. Noyori, *J. Am. Chem. Soc.* **1988**, *110*, 629; T. Ohkuma, M. Kitamura, R. Noyori, *Tetrahedron Lett.* **1990**, *31*, 5509.
[11] U. Ringeisen, 'Synthese und Charakterisierung von N-heterocyclischen Organophosphaten als Inhibitoren der Acetylcholinesterase', Ph.D. Thesis, University of Zurich, 1996.
[12] J. A. Dale, D. L. Dull, H. S. Mosher, *J. Org. Chem.* **1969**, *34*, 2543; G. R. Sullivan, J. A. Dale, H. S. Mosher, *J. Am. Chem. Soc.* **1973**, *38*, 2143; J. A. Dale, H. S. Mosher, *J. Am. Chem. Soc.* **1973**, *95*, 512; I. Ohtani, T. Kusumi, Y. Kahman, H. Kakisawa, *J. Am. Chem. Soc.* **1991**, *113*, 4092.
[13] C. Clerc, I. Matarazzo, P. Rüedi, *Helv. Chim. Acta* **2009**, *92*, 14.
[14] C. J. Shi, B. Zhou, A. S. Gopalan, W. R. Shieh, F. Van Middlesworth, in 'Selectivity – a Goal for Synthetic Efficiency', Workshop Conferences, Hoechst, Vol. 14, Eds. W. Bartmann, B. M. Trost, Verlag Chemie, Weinheim, 1983; J. C. Shi, C.-S. Chen, *Angew. Chem.* **1984**, *96*, 556; D. Seebach, S. Roggo, J. Zimmermann, 'Stereochemistry of Organic and Bioorganic Transformations', Workshop Conferences, Hoechst, Vol. 17, Eds. W. Bartmann, K. B. Sharpless, VCH-Verlagsgesellschaft, Weinheim, 1987; R. Csuk, B. Glänzer, *Chem. Rev.* **1991**, *91*, 49.
[15] C.-H. Wong, G. Whitesides, 'Enzymes in Synthetic Organic Chemistry' Pergamon, Oxford, 1995, p. 139.
[16] D. Seebach, V. Prelog, *Angew. Chem.* **1982**, *94*, 696.
[17] M. Kitamura, M. Tokunaga, T. Ohkuma, R. Noyori, *Tetrahedron Lett.* **1991**, *32*, 4163; K. Mashima, K. Kusano, N. Sato, Y. Matsumara, K. Nozaki, H. Kumobayashi, N. Sayo, Y. Hori, T. Ishizaki, S. Akutagawa, H. Takaya, *J. Org. Chem.* **1994**, *59*, 3064.
[18] R. Noyori, T. Okhuma, *Angew. Chem., Int. Ed.* **2001**, *40*, 40.
[19] R. Noyori, T. Ikeda, T. Ohkuma, M. Widhalm, M. Kitamura, H. Takaya, S. Akutagawa, N. Sayo, T. Saito, T. Taketomi, H. Kumobayashi, *J. Am. Chem. Soc.* **1989**, *111*, 9134; M. Kitamura, T. Ohkuma, M. Tokunage, R. Noyori, *Tetrahedron: Asymmetry* **1990**, *1*, 1; M. Kitamura, M. Tokunaga, R. Noyori, *J. Am. Chem. Soc.* **1993**, *115*, 144.
[20] S. Furegati, M. Binder, A. Linden, P. Rüedi, *Helv. Chim. Acta* **2006**, *89*, 1351.
[21] M. Wächter, ' Herstellung von optisch aktiven Organophosphaten mit *cis*- und *trans*-Decalingerüst zur Untersuchung der Inhibition von Acetylcholinesterase mittels Enzymkinetik und ^{31}P-NMR Spektroskopie', Ph.D. Thesis, University of Zurich, 2009.
[22] M. Wächter, S. Jurt, A. Linden, P. Rüedi, in preparation.
[23] S. E. Szedlacsek, R. G. Duggleby, *Methods Enzymol.* **1995**, *249*, 144.
[24] A. Baici, *Biol. Chem.* **1998**, *379*, 1007.
[25] I. H. Segel, 'Biochemical Calculations', Wiley, New York, 1976, p. 208; H. Bisswanger, 'Enzymkinetik', 3rd edn., VCH Publishers, Weinheim, 2000.
[26] A. Baici, P. Schenker, M. Wächter, P. Rüedi, *Chem. Biodiversity* **2009**, *6*, 261.
[27] A. R. Main, *Science (Washington, DC, U.S.)* **1964**, *114*, 992; G. Hart, R. D. O'Brien, *Biochemistry* **1973**, *12*, 2940.
[28] G. L. Ellman, K. D. Courtney, V. Andres Jr., R. M. Featherstone, *Biochem. Pharmacol.* **1961**, *7*, 88.
[29] M. Wächter, ' Herstellung optisch aktiver Organophosphate mit *cis*- und *trans*-Decalingerüst zur Untersuchung der Inhibition von Acetylcholinesterase', M. Sc. Thesis, University of Zurich, 2005.
[30] L. P. A. de Jong, H. P. Benschop, in 'Stereoselectivity of Pesticides', Eds. E. J. Ariens, J. J. S. van Rensen, W. Welling, Elsevier, Amsterdam, 1988, p. 109.
[31] G. Lambrecht, 'Struktur- und Konformations-Wirkungs-Beziehungen Heterocyclischer Acetylcholinanaloga', Habilitation Thesis, University of Frankfurt/M, 1979; N. J. Lewis, K. K. Barker, R. M. Fox Jr., M. P. Mertes, *J. Med. Chem.* **1973**, *16*, 156; S. Takemura, Y. Miki, F. Komada, K. Takahashi, A. Suzuki, *Chem. Pharm. Bull.* **1979**, *27*, 1893.
[32] J. L. Sussman, M. Harel, F. Frolow, C. Oefner, A. Goldman, L. Toker, I. Silman, *Science (Washington, DC, U.S.)* **1991**, *253*, 872; G. Koellner, G. Kryger, C. B. Millard, I. Silman, J. L. Sussman. T. Steiner, *J. Mol. Biol.* **2000**, *296*, 713.
[33] D. R. Ripoll, C. H. Faerman, P. H. Axelsen, I. Silman, J. L. Sussman, *Proc. Natl. Acad. Sci. U.S.A.* **1993**, *90*, 5128.

[34] A. N. Pryor, T. Selwood, L.-S. Leu, M. A. Andracki, B. H. Lee, M. Rao, T. Rosenberry, B. P. Doctor, I. Silman, D. M. Quinn, *J. Am. Chem. Soc.* **1992**, *114*, 3897; D. R. Ripoll, C. H. Faerman, P. H. Axelsen, I. Silman, J. L. Sussman, *Proc. Natl. Acad. Sci. U.S.A.* **1993**, *90*, 5128; M. Harel, I. Schalk, L. Ehret-Sabatier, F. Bouet, M. Goeldner, C. Hirth, P. H. Axelsen, I. Silman, J. L. Sussman, *Proc. Natl. Acad. Sci. U.S.A.* **1993**, *90*, 9031.
[35] Y. Bourne, Z. Radić, G. Sulzenbacher, E. Kim. P. Taylor, P. Marchot, *J. Biol. Chem.* **2006**, *281*, 29256, and refs. cit. therein.
[36] F. G. Canepa, P. J. Pauling, H. Sörum, *Nature (London)* **1966**, *210*, 907; C. Chothia, P. Pauling, *Nature (London)* **1968**, *219*, 1156; M. Sax, M. Rodrigues, G. Blank, M. K. Wood, J. Pletcher, *Acta Crystallogr., Sect. B* **1976**, *32*, 1953.
[37] P. Partington, J. Feeny, A. S. V. Burgen, *Mol. Pharmacol.* **1972**, *8*, 269.
[38] C. J. Wilkins, *J. Chem. Soc.* **1951**, 2726.
[39] R. Hooft, KappaCCD Collect Software, Nonius BV, Delft, The Netherlands, 1999.
[40] Z. Otwinowski, W. Minor, in 'Methods in Enzymology', Vol. 276, 'Macromolecular Crystallography', Part A, Eds. C. W. Carter Jr., R. M. Sweet, Academic Press, New York, 1997, p. 307.
[41] R. H. Blessing, *Acta Crystallogr., Sect A* **1995**, *51*, 33.
[42] A. Altomare, G. Cascarano, C. Giacovazzo, A. Guagliardi, M. C. Burla, G. Polidori, M. Camalli, SIR92, *J. Appl. Crystallogr.* **1994**, *27*, 435.
[43] A. H. Spek, PLATON, Program for the Analysis of Molecular Geometry, University of Utrecht, The Netherlands, 2005.
[44] H. D. Flack, G. Bernardinelli, *Acta Crystallogr., Sect A* **1999**, *55*, 908; H. D. Flack, G. Bernardinelli, *J. Appl. Crystallogr.* **2000**, *33*, 1143.
[45] E. N. Maslen, A. G. Fox, M. A. O'Keefe, in 'International Tables for Crystallography', Ed. A. J. C. Wilson, Kluwer Academic Publishers, Dordrecht, 1992, Vol. C, Table 6.1.1.1, p. 477.
[46] R. F. Stewart, E. R. Davidson, W. T. Simpson, *J. Chem. Phys.* **1965**, *42*, 3175.
[47] J. A. Ibers, W. C. Hamilton, *Acta Crystallogr.* **1964**, *17*, 781.
[48] D. C. Creagh, W. J. McAuley, in 'International Tables for Crystallography', Ed. A. J. C. Wilson, Kluwer Academic Publishers, Dordrecht, 1992, Vol. C, Table 4.2.6.8, p. 219.
[49] D. C. Creagh, J. H. Hubbell, in 'International Tables for Crystallography', Ed. A. J. C. Wilson, Kluwer Academic Publishers, Dordrecht, 1992, Vol. C, Table 4.2.4.3, p. 200.
[50] G. M. Sheldrick, SHELXL97, Program for the Refinement of Crystal Structures, University of Göttingen, Germany, 1997.
[51] C. K. Johnson, ORTEPII, Report ORNL-5138, Oak Ridge National Laboratory, Oak Ridge, Tennessee, 1976.

Received December 16, 2010